Editor Decision: Publish subject to minor revisions (review by editor) (04 Feb 2019) by Monica Bini

Comments to the Author:

The authors made a good job in the review of the manuscript.

Few minor revisions are still required before the acceptance for publication:

Line 403: please, in order to be consistent with the text and the special issue, change "4400-4000" whit "4.4-4.0 ka BP"

Line 741 "Gulf of Omen" is "Gulf of Oman"

After these changes the manuscript will be accepted.

Reply: Thank you very much for your affirmation and comments.

We have changed "4400-4000" with "4.4-4.0 ka BP", and changed "Gulf of Omen" with "Gulf of Oman". Line 402 and Line 735.

Physical processes of cooling and megadrought in 4.2 ka BP event: results from TraCE-21ka simulations

Mi Yan[1,2], Jian Liu[1,2,3*]

[1]Key Laboratory for Virtual Geographic Environment of Ministry of Education/State Key Laboratory of Geographical Evolution of Jiangsu Provincial Cultivation Base/School of Geography Science, Jiangsu Center for Collaborative Innovation in Geographical Information Resource Development and Application, Nanjing Normal University, Nanjing 210023, China

[2]Open Studio for the Simulation of Ocean-Climate-Isotope, Pilot National Laboratory for Marine Science and Technology, Qingdao 266237, China

[3]Jiangsu Provincial Key Laboratory for Numerical Simulation of Large Scale Complex Systems/School of Mathematical Science, Nanjing Normal University, Nanjing 210023, China Key Laboratory of Virtual Geographic Environment, Ministry of Education; State key Laboratory of Geographical Environment Evolution, Jiangsu Provincial Cultivation Base; School of Geographical Science, Nanjing Normal University, Nanjing, 210023, China

[2]Jiangsu Center for Collaborative Innovation in Geographical Information Resource Development and Application, Nanjing, 210023, China

*jliu@njnu.edu.cn

Abstract

It is widely believed that multidecadal to centennial cooling and drought occurred from 4500 BP to 3900 BP, known as the 4.2 ka BP event that triggered the collapse of several cultures. However, whether this event was a global event or a regional event and what caused this event remain unclear. In this study, we investigated the spatiotemporal characteristics, the possible causes and the related physical processes of the event using a set of long-term climate simulations, including one all-forcing experiment and four single-forcing experiments. The results derived from the all-forcing experiment show that this event occurs over most parts of the Northern Hemisphere (NH), indicating that this event could have been a hemispheric event. The cooler NH and warmer Southern Hemisphere (SH) illustrate that this event could be related to the slowdown of the Atlantic Meridional Overturning Circulation (AMOC). The comparison between the all-forcing experiment and the single-forcing experiments indicates that this event might be caused by internal variability, while external forcings such as orbital and greenhouse gases might have modulation effects. A positive North Atlantic Oscillation (NAO)-like pattern in the atmosphere (low troposphere) triggered a negative Atlantic Multidecadal Oscillation (AMO)-like pattern in the ocean, which then triggered a Circumglobal Teleconnection (CGT)-like wave train pattern in the atmosphere (high troposphere). The positive NAO-like pattern and the CGT-like pattern are the direct physical processes that lead to the NH cooling and megadrought. The AMO-like pattern plays a "bridge" role in maintaining this barotropic structure in the atmosphere at a multidecadal-centennial time scale. Our work provides a global image and dynamic background to help better understand the 4.2 ka BP event.

1 Introduction

Understanding the characteristics and mechanisms of climate changes during the Holocene can help predicting future changes. The multidecadal-to-centennial abrupt climate change, or the rapid climatic change during ca. 4.5-3.9 ka BP (before 1950 CE), the so called "4.2 ka BP event", was one of the major climate events during the Holocene (Wang, 2009; Staubwasser and Weiss, 2006; Mayewski et al., 2004; Wang, 2010). This event is considered to be closely linked to the cultural evolutions of different regions of Eurasia such as the collapse of the Akkadian empire, the termination of the urban Harappan civilization in the Indus valley and the collapse of Neolithic Cultures around the Central Plain of China (Weiss et al., 1993; Weiss and Bradley, 2001; Wu and Liu, 2001; Staubwasser et al., 2003; Wu and Liu, 2004; An et al., 2005; Staubwasser and Weiss, 2006; Liu et al., 2013; Weiss, 2015, 2016). Moreover, this event is also thought to be the transition of the Middle to Late Holocene (Walker et al., 2012; Finkenbinder et al., 2016). However, the characteristics, causes and corresponding mechanisms behind this event remain unclear.

The 4.2 ka BP event is mostly characterized by rapid events at various latitudes (Jansen et al., 2007), e.g., cooling in Europe (Lauritzen, 2003), centennial megadroughts in North America (Booth et al., 2005), decreased precipitation in both southern and northern China (Tan et al., 2008), and the weakened summer monsoon in India (Nakamura et al., 2016); however, the manifestation of this event is far from convincing and needs more evidence and simulation investigations (Roland et al., 2014). Many reconstructions have shown that the 4.2 ka BP event is dominated by megadroughts at centennial-scale over mid-low latitudes (Tan et al., 2008; Yang et al., 2015; Weiss, 2016). However, Roland et al. (2014) found no compelling evidence, at least in peatland records, to support that there was a 4.2 ka BP event in Great Britain and Ireland. Moreover, according to the hydrologic cycle (i.e. the hydroclimate changes are often regionally specific), it cannot be ruled out that there were no flooding events somewhere else during this period. For example, Huang et al. (2011) and Tan et al. (2018) found that successive floods occurred over the middle reaches of the Yellow River in China in association with the abrupt climatic event of 4.2 ka BP.

Understanding the causes and mechanisms of the 4.2 ka BP event can provide explanations for the reconstructed discrepancies over different regions. For the causes of the event, some reconstruction and modeling studies have suggested that the solar irradiance could have played an important role in the early Holocene climate changes (Wang et al., 2005; Rupper et al., 2009; Owen and Dortch, 2014); however, no strong evidence has shown that the solar irradiance affected glacier fluctuations (cooling events) in the late Holocene since there is yet no good mechanistic explanations of how small changes in solar irradiance could significantly affect large scale climate changes (Solomina et al., 2015). Tan et al. (2008) thought that the 4.2 ka BP event could have been induced by the southward shift of the Intertropical Convergence Zone (ITCZ) and oceanic sea surface temperature (SST) changes, as well as the vegetation feedback caused by the solar activity. Liu et al. (2013) and Deininger et al. (2017) argued that the atmospheric circulation, such as the North Atlantic Oscillation (NAO)-like pattern but on a centennial time scale, could have played a more important role than the ocean circulation in this event, although the mechanisms that forced the circulation change remained unclear. A new reconstruction study has also shown that the dry phases over the western Mediterranean in the period of 4.5 ka BP-2.8 ka BP generally agreed with positive NAO conditions (Ramos-Román et al., 2018). However, studies come to different conclusions on the likely phase of the NAO-like patter during the late Holocene (Finkenbinder et al., 2016). Some studies show positive NAO-type patterns during the late Holocene (Tremblay et al., 1997; Sachs, 2007; Ramos-Román et al., 2018), whereas others show negative NAO-like patterns (Rimbu et al., 2004). Since the mechanisms could be a complex set of air-sea interactions (Roland et al., 2014), it is hard for reconstruction to provide a general record due to its limitations such as interpretation and spatially incompleteness. The mechanisms behind the 4.2 ka BP event need to be clarified.

Therefore, to improve understanding of the 4.2 ka BP event, new high-resolution reconstruction studies that focus on the 4.2 ka BP event are required. On the other hand, physical-based modeling research can provide general concepts of the characteristics of the event along with the causes and the mechanisms. Climate simulations have been conducted to investigate another abrupt cooling event in the early Holocene, the so-called 8.2 ka BP event. The simulations were used to test the hypothesis raised by the reconstruction studies that the 8.2 ka BP event was most likely caused by freshwater forcing and was associated with weakening of the Atlantic Meridional Overturning Circulation (AMOC) (Morrill et al., 2013; Wagner et al., 2013; Morrill et al., 2014; Matero et al., 2017; Ljung et al., 2008; Alley and Agustsdottir, 2005). For example, the simulations argued that the meltwater from the collapse of the ice dome over Hudson Bay was an essential forcing of the 8.2 ka BP event (Wagner et al., 2013; Matero et al., 2017). However, little modeling work has been applied to the 4.2 ka BP event.

Recently, Ning et al. (2019) briefly compared the spatial patterns of climate change in the 9th and 5th millennia BP using a set of transient modeling results on a long-term perspective. In the present study, we will use the same set of simulation results to provide an in-depth characteristics of the 4.2 ka BP event and will focus on the possible causes and mechanisms behind this event. The model and experiments are introduced in Sect. 2. The results are shown in Sect. 3. The possible causes and mechanisms are discussed in Sect. 4, and conclusions are drawn in Sect. 5.

2 Model and experiments

A set of transient simulations (TraCE-21ka, Simulation of Transient Climate Evolution over the past 21,000 years, He, 2011) conducted with the Community Climate System model version 3 (CCSM3) was used to investigate the spatial and temporal characteristics of the 4.2 ka BP event and to determine the possible causes and mechanisms behind this event. The experiments are listed in Table 1, including one transient experiment with all-forcings (TraCE-ALL), one single-forcing experiment forced only by transient orbital variation (TraCE-ORB), one single-forcing experiment forced only by transient melt-water flux (TraCE-MWF), one single-forcing experiment forced only by quasi-transient ice-sheet (TraCE-ICE), and one single-forcing experiment forced only by transient greenhouse gases concentrations changes (TraCE-GHG). The simulations were conducted from 22000 BP to 1990 CE for the TraCE-ALL, the TraCE-ORB and the TraCE-GHG experiments, and from 19000 BP to 1990 CE for the TraCE-MWF and the TraCE-ICE experiments.

The transient June insolation changes at 60°N and 60°S that resulted from the orbital variation and the transient CO_2 change used in the simulations are shown in Fig. 1. The continental ice-sheet and topography changes are based on the ICE-5G (VM2) reconstruction (He et al., 2013; Peltier, 2004). For the geography changes, the Barents Sea opens at 13.1 ka BP, the Bering Strait opens at 12.9 ka BP, Hudson Bay opens at 7.6 ka BP, and the Indonesian Throughflow opens at 6.2 ka BP. The freshwater injected into Northern Hemisphere (NH) and Southern Hemisphere (SH) oceans are based on specific time slices (e.g., 19 ka BP into North Atlantic, 17 ka BP into North Atlantic, 11.5 ka BP into Arctic, St. Lawrence River, Hudson Strait, Barents Sea, North Sea, Ross Sea and Weddell Sea). Note that no freshwater was delivered to the ocean after 5000 BP in the TraCE-ALL and TraCE-MWF experiments. The detailed information about the experiments design can be referred to He (2011) and He et al. (2013).

The TraCE-21ka simulation was evaluated with reconstructions and was found that it could reproduce major deglacial temperature evolutions (Clark et al., 2012; Shakun et al., 2012). It has been used to depict the causes and mechanisms of Holocene climate changes, such as the Bølling-Allerød warming (Liu et al., 2009), cooling into the Younger Dryas and recovery to warm conditions (Liu et al., 2012) and the ENSO evolution over the past 21 ka (Liu et al., 2014a). In the present work, we adopted the period of 5000 BP-3000 BP to focus on the 4.2 ka BP event.

3 Results

3.1 Identification of 4.2 ka BP event in the model simulation

The 101-year running mean annual NH surface temperature and precipitation during 5 ka BP-3 ka BP shows double peak centennial cooling and drought from 4.4 ka BP to 4.0 ka BP (Fig. 2, dashed black line). However, the variabilities are smaller over the SH than those over the NH. There is no significant cooling and drought event during that period (Fig. S1, dashed black line) over the SH. The SH precipitation even shows a double-peak wet condition during the period of 4.4 ka BP-4.0 ka BP.

The double peak centennial cooling and drought are still obvious when the 31-year running mean is applied to the time series (not shown), which indicates that the simulated climate events potentially comparable to the 4.2 ka event. Moreover, the centennial warming periods right before and after the cooling event indicate that this event might be included in a quasi-millennium variation. Therefore, the 4.2 ka BP event could be a multiscale event, i.e. from multi-decadal to millennium.

The seasonal mean NH surface temperature changes show that the annual mean variability is dominated by the boreal winter (December-January-February, DJF) surface temperature change (Fig. S2). The correlation coefficient between the annual mean NH surface temperature (NHT) and the DJF mean NHT is 0.96 (after the 101-year running mean), which is significant above the 99% confidence level, much higher than the correlation coefficient between the annual mean and the boreal summer (June-July-August, JJA) mean of only 0.30 (after the 101-year running mean), which is not significant. However, this is different for the precipitation change, for which both the JJA mean and the DJF mean contribute to the annual mean precipitation change (not shown).

To identify the characteristics of the 4.2 ka BP event, two centennial cool periods and two centennial warm periods that exceeded ±0.5 standard deviations are selected. The two centennial cool periods span from 4320 BP to 4220 BP and from 4150 BP to 4050 BP, and the two centennial warm periods span from 4710 BP to 4610 BP and from 3980 BP to 3880 BP.

3.2 Spatial characteristics of surface temperature and precipitation

To help draw a coherent global view of the 4.2 ka BP event, the spatial characteristics of temperature and precipitation changes during the 4.2 ka BP event are shown in Fig. 3.

Figure 3a gives the spatial distribution of the annual mean surface temperature difference between the cold periods and the warm periods. The cooling significantly occurred over most regions of the NH, especially over the middle to high latitudes of the NH and most land regions of the SH. Most parts of India, northern Mexico and the middle latitudes of the SH ocean experienced warm conditions. Such asymmetric change between the hemispheres (cool NH and warm SH) favors the southward shift of the ITCZ. The spatial distribution of the surface temperature change is still dominated by the boreal winter pattern (not shown). The large cooling over the NH and small warming over the SH could be related to the orbital change (Fig. S3), which induces insolation increasing over the SH but decreasing over the NH.

The spatial distribution of annual mean precipitation differences between the cold periods and the warm periods is shown in Fig. 3b. During the cold periods, significant drought is mainly located over many land regions of the NH, especially over Europe, western Asia, and interior North America and Central America. The significant dry conditions over the Dead Sea, the Gulf of Omen, interior North America and western North Africa and the wet condition over South America are consistent with the reconstructions (Yechieli et al., 1993; Cullen et al., 2000; Forman et al., 1995; Marchant and Hooghiemstra, 2004). For the SH, the land precipitation increased, which indicates a southward shift of the ITCZ, as suggested by the aforementioned asymmetric temperature change and by the previous studies based on both reconstructions (Fleitmann et al., 2007; Cai et al., 2012) and simulations (Broccoli et al., 2006). Over East China, the precipitation anomalies show a wet south-dry north pattern, which indicates a weakened East Asian monsoon revealed by the reconstruction record (Tan et al., 2018). However, the simulated anomaly pattern is not very significant over East China. This might be related to the model resolution, the model performance, or the actual climate change. Therefore, simulations with higher resolution, inter-model and model-data comparisons are required to draw a clearer view about the climate change over East China.

The sea surface temperature (SST) shows that the largest change occurs over the northern Atlantic Ocean and then the northern Pacific Ocean (Fig. 4). The warmer south and cooler north over the Atlantic Ocean indicates an Atlantic Multi-Decadal Oscillation (AMO)-like pattern with its cold phase. The cold phase of the AMO has been confirmed to induce summer rainfall decreases over India and Sahel in both simulations and proxy data (Zhang and Delworth, 2006; Shanahan et al., 2009).

The simulated characteristics of the temperature change, the precipitation change, and the SST change are similar to those responses to the weakened AMOC state (Vellinga and Wood, 2002; Zhang and Delworth, 2005; Delworth and Zeng, 2012; Brown and Galbraith, 2016) (Fig. S4).

3.3 Circulations associate with the 4.2 ka BP event

The sea level pressure (SLP) differences between the cooler periods and the warmer periods show that the largest change occurs over the mid-high latitudes of the NH and SH (Fig. 5a). The negative SLP anomalies over the high North Atlantic and positive SLP anomalies over the middle North Atlantic during the cool periods resemble a positive North Atlantic Oscillation (NAO)-like pattern but on a centennial-millennial time scale. The positive NAO-like pattern is accompanied by cyclonic circulation over Iceland and anticyclonic circulation over the Azores Islands and thus strengthened westerlies over the downstream regions (Fig. 5a). The subtropical highs and the relative anticyclones in both the SH and NH are strengthened during the cold periods from low troposphere (850 hPa) to high troposphere (200 hPa), which illustrates a barotropic structure (Fig. 5). Note that the strengthened subtropical highs over the NH are most significant at low level (sea level and 850 hPa), while the subtropical highs over the SH are most significant at high level (200 hPa). The centers with positive geopotential height anomalies during the 4.2 ka BP event over Western Europe, Central Asia, East Asia, the east north Pacific and Eastern North America, as well as the anti-cyclonic circulation anomalies at 200 hPa (Fig. 5d), resemble a Circumglobal Teleconnection (CGT)-like wave pattern (Ding and Wang, 2005; Lin et al., 2016) but on a centennial-millennial time scale.

The strengthened subtropical highs with mid-latitudes anticyclones from lower to upper levels are the direct physical processes that cause the precipitation decreases and thus the following megadrought over mid-latitudes of NH regions, particularly over Eurasia. The cooler land-warmer ocean over East Asia and the West Pacific (Fig. 3a) indicate weakened land-ocean thermal contrast associated with significantly higher SLP over land and lower SLP over the adjacent ocean (insignificant) (Fig. 5a). The weakened land-ocean contrast can lead to a weaker East Asian monsoon, accompanied by precipitation increases over the southern China pattern and precipitation decreases over the northern China pattern (Fig. 3b). Such conclusion is very rough, since the simulated anomaly patterns are not very significant. More investigations with higher resolutions of modeling and reconstruction works are required to get satisfactory results.

4 Discussions

The simulations show that the cool and dry conditions of the 4.2 ka BP event is more like a hemispheric phenomenon, mainly located over the NH, rather than a global phenomenon. The land over the SH experiences cool but wet conditions, and the mid-latitude SH ocean is warmer. The potential causes and mechanisms of this event will be discussed in this section.

4.1 The possible causes of the 4.2 ka BP event

Some records suggested that solar irradiance was one of the essential mechanisms that drove the Holocene climate variation at centennial to millennial time scales (Bond et al., 2001), whereas others suggested that the linkage between solar irradiance and multicentury scale cooling events during the Holocene was weak, particularly in the mid- to late-Holocene (Turney et al., 2005; Wanner et al., 2008). Changes in solar irradiance are not included in the experiments used in the present work. Nonetheless, we still obtain multicentury cooling events (such as the 4.2 ka BP event) in the TraCE-ALL experiment, but with smaller magnitude. This side-fact indicates that the solar irradiance might not be the driving factor for the Holocene cooling events.

If the results derived from the TraCE-ALL experiment are consistent with those derived from a particular single-forcing sensitivity experiment, we assume the variation to be forced by that forcing. Otherwise, if the results derived from the TraCE-ALL experiment differ from those from the single-forcing sensitivity experiments, we assume the variation to be forced by the internal variability. In this section, we use the series after applications of 101-year running means as an example and compare the results derived from the all-forcing experiment to those derived from the single-forcing experiment to determine the possible forcings that triggered the 4.2 ka BP event.

The correlation coefficients between the annual mean NHT derived from the

TraCE-ALL run and the NHT derived from each single-forcing run are listed in Table 2. A two-sided Students t-test is used for the statistical significant test, assuming 20 degrees of freedom, which is estimated simply from a 2000-year time series subjected to a 100-year running mean (Delworth and Zeng, 2012). There is no significant clue that the annual mean NHT variation is forced by the orbital variation or the other forcings due to the non-significant correlations. During the period of 5000 BP - 3000 BP, the variation of simulated JJA mean NHT is likely forced by the solar radiation due to the orbital variation (Table 2; the correlation coefficient between the two series is 0.79 at $p<0.05$), whereas the greenhouse gas change has a comparable negative impact on the JJA mean NHT (the correlation coefficient is -0.73 at $p<0.05$). The melt-water flux also has a moderate contribution to the JJA mean NHT change (the correlation coefficient is 0.48 at $p<0.05$). For the DJF mean NHT, only melt-water flux has a notable negative effect (the correlation coefficient is -0.43 at $p<0.05$). However, there is no meltwater forcing during this period, so the NHT change can be taken as internal variability. Therefore, the significant correlation coefficient between the all forcing run result and the meltwater forcing run result might be a coincidence, due to the autocorrelation of internal variability. This is another side-fact indicating the cold events during the late Holocene might be related to the internal variability. Note that if the effective degree of freedom is used, none of the abovementioned correlation coefficients are significant. The effective degree of freedom is calculated by the following equation:

$$N_{dof} = N \times \frac{1 - r1 \times r2}{1 + r1 \times r2}$$

where N_{dof} is the effective degree of freedom regarding to the two correlation samples, N is the total sample size, r_1 and r_2 are autocorrelation lag-1 values for sample 1 and sample 2, respectively (Bretherton et al., 1999).

On the other hand, the annual mean NHT difference between the TraCE-ALL run and the sum of the 4 single-forcing sensitivity experiments shows variation similar to the NHT derived from the TraCE-ALL run from 5000 BP to 3000 BP (Fig. S5). The correlation coefficient between these two time-series is 0.66, which is significant above the 95% confidence level (assuming 20 degrees of freedom). We assume the difference between the TraCE-ALL run and the sum of the 4 single forcing runs to be the internal variation, taking that the climate responses to the external forcings are linear at global and hemispheric scales. Therefore, the internal variation might play a dominant role in the climatic variation during the period of 5000 BP-3000 BP. However, the linearity of the climate responding to the external forcings need further clarification, since there would be interactions between each forcing and between forcings and internal variability.

Moreover, there is no double-peak cooling event during the period of 4400 BP-4000 BP in any single forcing run (Fig. 1, colored lines), which indicates that the 4.2 ka BP event might not be triggered by those external forcings, including the orbital, the melt-water flux, the ice-sheets and the greenhouse gases in isolation. Volcanic eruptions have been identified as one of the important drivers of climate variation, whereas there were few eruptions during 4400 BP-4000 BP (Sigl et al., 2018). Therefore, we conclude that the variability relating to the 4.2 ka BP event might be driven by the internal variability. Klus et al. (2017) also suggested that the internal climate variability could trigger abrupt cold events in the North Atlantic without external forcings (e.g., solar irradiance or volcanic).

However, why such large variation due to the internal variability occurs at approximately 4.2 ka BP remains unknown. There is little ice-sheet change and no melt water discharge after 5.0 ka BP in the TraCE-ICE run and TraCE-MWF run, and the variations of climate derived from these two runs can thus be considered as internal variabilities. The multicentennial cooling events can also be found in the standardized NHT during the last 5000 years of the two experiments (Fig. S6), and there are drought events in the standardized NH precipitation time series (not shown). However, the timing of those cooling and drought events occurs stochastically. This indicates a general concept of the random variation of the internal mode of the climate system. There is a reduction of NH temperature and precipitation at around 4600 BP in the TraCE-ORB (Fig. 2, orange lines), which might be related to the timing of the event as speculated by Ning et al. (2019).

Ning et al. (2019) compared the 5th millennium BP cooling with the 9th millennium cooling and concluded that the 9th millennium BP cooling was resulted from the freshwater forcing while the orbital forcing is the most likely explanation of cooling in the North Atlantic starting from the early 5th Millennium BP through most of the later Holocene, but with fluctuations. In the present work, we attribute this fluctuation to the internal variability, which is superposed on the orbital induced long-term trend. This work and Ning et al.'s work (2019) focus on different aspects and different time scales, and are complementary to better understand the 4.2 ka BP event.

4.2 The mechanisms of the centennial-millennial cooling and drought

As has mentioned in Sec. 3.3, the low level NAO-like pattern and upper level CGT-like pattern are the direct mechanisms that cause cooling and megadroughts over most part of the NH. Previous studies also proposed that the temperature and precipitation changes over Eurasia and Africa were directly linked to the NAO (Cullen et al., 2002; Kushnir and Stein, 2010). The first leading mode of the Empirical Orthogonal Function (EOF) of the annual mean SLP during 5 ka BP-3 ka BP shows a double-peak positive NAO-like pattern but on a centennial scale during the period of 4400 BP-4000 BP (Fig. 6). The first leading EOF of geopotential height at 200 hPa after application of a 31-year running mean shows a CGT-like pattern and similar double-peak variation during the period of 4400 BP-4000 BP, which is more obvious after applying the 101-year running mean (Fig. 7). This means that the double-peak cooling and drought of the 4.2 ka BP event could be strongly related to the double peak positive NAO-like pattern (at low level) and CGT-like pattern (at high level) at a centennial time scale.

Li et al. (2013) suggested that the NAO is a predictor of NHT multidecadal variability during the 20th century. In this study, significant correlation is also found between the annual mean NAO index and the annual mean NHT during the period of 4400 BP-4000 BP, with the NAO leading by approximately 40 years (Fig. 8). The NAO index is defined by the first leading mode of the EOF of the SLP. The regressed annual mean surface temperature against the NAO index 40 years earlier during 4400 BP and

4000 BP shows cooler NH high latitudes and a warmer SH (Fig. S7), especially the cooling over the northern North Atlantic Ocean, Europe, East Asia and North America.

The geopotential height at 200 hPa regressed against the SST over the two North Atlantic outstanding regions (Fig. 4) shows a CGT-like pattern after application of a 31-year running mean (Fig. 9), which is similar to the conclusion from Lin et al. (2016) that the CGT could be excited by the AMO-related SST anomaly. The regressed 200 hPa geopotential height shows a similar pattern after application of a 101-year running mean (not shown). The anticyclones associated with CGT-like pattern over the West Europe, Central Asia and North America can suppress the precipitation and thus lead to megadrought over these regions.

Considering the NAO-like pattern, the CGT-like pattern and the AMO-like pattern together, we suggest that the AMO could be playing a "bridge" role to keep the barotropic structure at the centennial scale, which is similar to the synthesis proposed by Li et al. (2013) that the AMO is a "bridge" that links the NAO and NHT at a multidecadal timescale. Delworth and Zeng (2016) suggested that the NAO variation had significant impact on the AMOC and the subsequent influence on the atmosphere and large-scale climate at multidecadal-centennial time scales. Other studies also focused on the role of SST anomalies over the North Pacific and North Atlantic oceans when investigating the possible mechanisms of the 4.2 ka BP event (Kim et al., 2004; Marchant and Hooghiemstra, 2004; Booth et al., 2005).

We notice the centennial-millennial variation of the AMOC after the mid-Holocene in the all forcing run (Fig. S4a). There also exits a double peak variation during the period of 4.4~~00~~-4.0~~00~~ ka BP, accompanied by the similar spatial patterns of temperature and precipitation anomalies as the simulated 4.2 ka BP event (Fig. S4b, c). However, whether this AMOC variation is related to the external forcing, such as the orbital forcing, or just the internal variability remains unknown, and needs further investigations.

5 Conclusion

The characteristics of the 4.2 ka BP event along with the potential drivers and the mechanisms are investigated using a set of transient climate simulations. The simulated event is characterized by hemispheric cooling and megadrought over the NH, whereas the SH experiences warming (over mid-latitude ocean) and wet conditions during this event. The annual mean temperature change is dominated by the boreal winter change. The cool and dry NH and warm and wet SH pattern indicates a southward shift of the ITCZ, as suggested by the reconstructions. These characteristics could also be related to a weakening of the AMOC, which needs further investigation.

By comparison between the all-forcing experiment and the single-forcing sensitivity experiments, the 4.2 ka BP event can largely be attributed to the internal variability, although the orbital forcing and the greenhouse gases could impact the boreal summer NHT variation. The origin could be in polar regions and the North Atlantic and may influence the NH climate through teleconnections such as the NAO-like pattern and the CGT-like pattern. The positive NAO-like pattern in the atmosphere triggers cooling over the NH and the negative AMO-like pattern in the ocean, which may last for decades or even centuries. The negative AMO-like pattern triggers CGT-like wave patterns at a multidecadal-centennial time scale accompanied by anticyclones over West Europe, Central Asia and North America, which induce megadrought over those regions. The simplified diagram of the mechanism is shown in Fig. 10.

Our findings provide a global pattern and mechanical background of the 4.2 ka BP event that can help better understanding this event. We attribute the internal variabilities to be an essential forcing of the 4.2 ka BP event. However, whether or not the external forcings have modulation effects need to be clarified. For example, is the timing of the event stochastic due to the internal variability or modulated by the external forcings such as the orbital changes? Why the SST forcing in the North Atlantic can be maintained at a multidecadal-centennial time scale requires more study. Current results are mainly based on annual mean precipitation and temperature, whereas the impacts of external forcings may have seasonal dependence; further investigations are required to evaluate these impacts.

The model responses to the external forcings are small, especially in the Holocene because of the absence of a significant change of the AMOC and the meltwater forcing after 6 ka (Liu et al., 2014b). So we use the amplified anomalies between the cold and warm periods, rather than simply the cold anomalies against the long-term average, to illustrate the mechanisms of the event. We need to keep in mind that we still might not be modeling the events comparable to the 4.2 ka BP event, particularly during the late Holocene. More model-data, inter-model and inter-events comparisons are required to better understand the cold events during the Holocene.

Acknowledgments

We acknowledge Prof. Bin Wang and two anonymous referees for the comments helping to clarify and improve the paper. This research was jointly supported by the National Key Research and Development Program of China (grant no. 2016YFA0600401), the National Basic Research Program (grant no. 2015CB953804), the National Natural Science Foundation of China (grant nos. 41671197, 41420104002 and 41631175), Open Funds of State Key Laboratory of Loess and Quaternary Geology, Institute of Earth Environment, CAS (SKLLQG1820), and the Priority Academic Development Program of Jiangsu Higher Education Institutions (PAPD, grant no. 164320H116). TraCE-21ka was made possible by the DOE INCITE computing program, and supported by NCAR, the NSFP2C2 program,and the DOE Abrupt Change and EaSM programs.

References:

Alley, R., and Agustsdottir, A.: The 8k event: cause and consequences of a major Holocene abrupt climate change, Quaternary Science Reviews, 24, 1123-1149, 10.1016/j.quascirev.2004.12.004, 2005.

An, C.-B., Tang, L., Barton, L., and Chen, F.-H.: Climate change and cultural response around 4000 cal yr B.P. in the western part of Chinese Loess Plateau, Quaternary Research, 63, 347-352, 10.1016/j.yqres.2005.02.004, 2005.

Bond, G., Kromer, B., Beer, J., Muscheler, R., Evans, M. N., Showers, W., Hoffmann, S., Lotti-Bond, R., Hajdas, I., and Bonani, G.: Persistent solar influence on North Atlantic climate during the Holocene, Science, 294, 2130, 2001.

Booth, R. K., Jackson, S. T., Forman, S. L., Kutzbach, J. E., Bettis, I. E. A., Kreig, J., and Wright, D. K.: A severe centennial-scale drought in mid-continental North America 4200 years ago and apparent global linkages, The Holocene, 15, 321-328, 2005.

Bretherton, C. S., Widmann, M., Dymnikov, V. P., Wallace, J. M., and Bladé, I.: The effective number of spatial degrees of freedom of a time-varying field, J. Climate, 12(7), 1990-2009, 1999.

Broccoli, A. J., Dahl, K. A., and Stouffer, R. J.: Response of the ITCZ to Northern Hemisphere cooling, Geophysical Research Letters, 33, L01702, 10.1029/2005gl024546, 2006.

Brown, N., and Galbraith, E. D.: Hosed vs. unhosed: interruptions of the Atlantic Meridional Overturning Circulation in a global coupled model, with and without freshwater forcing, Climate of the Past, 12, 1663-1679, 10.5194/cp-12-1663-2016, 2016.

Cai, Y., Zhang, H., Cheng, H., An, Z., Lawrence Edwards, R., Wang, X., Tan, L., Liang, F., Wang, J., and Kelly, M.: The Holocene Indian monsoon variability over the southern Tibetan Plateau and its teleconnections, Earth and Planetary Science Letters, 335-336, 135-144, 10.1016/j.epsl.2012.04.035, 2012.

Clark, P. U., Shakun, J. D., Baker, P. A., Bartlein, P. J., Brewer, S., Brook, E., Carlson, A. E., Cheng, H., Kaufman, D. S., Liu, Z., Marchitto, T. M., Mix, A. C., Morrill, C., Otto-Bliesner, B. L., Pahnke, K., Russell, J. M., Whitlock, C., Adkins, J. F., Blois, J. L., Clark, J., Colman, S. M., Curry, W. B., Flower, B. P., He, F., Johnson, T. C., Lynch-Stieglitz, J., Markgraf, V., McManus, J., Mitrovica, J. X., Moreno, P. I., and Williams, J. W.: Global climate evolution during the last deglaciation, Proceedings of the National Academy of Sciences of the United States of America, 109, E1134-1142, 10.1073/pnas.1116619109, 2012.

Cullen, H. M., Kaplan, A., Arkin, P. A., and DeMenocal, P. B.: Impact of the North Atlantic Oscillation on Middle Eastern climate and streamflow, Climatic Change, 55, 315-338, 2002.

Cullen, H., deMenocal, P., Hemming, S., Hemming, G., Brown, F. H., Guilderson, T., and Sirocko, F.: Climate change and the collapse of the Akkadian empire: Evidence from the deep sea, Geology, 28, 379-382, 2000.

Deininger, M., McDermott, F., Mudelsee, M., Werner, M., Frank, N., and Mangini, A.: Coherency of late Holocene European speleothem δ18O records linked to North Atlantic Ocean circulation, Climate Dynamics, 49, 595-618, 10.1007/s00382-016-3360-8, 2017.

Delworth, T. L., and Zeng, F.: Multicentennial variability of the Atlantic meridional overturning circulation and its climatic influence in a 4000 year simulation of the GFDL CM2.1 climate model, Geophysical Research Letters, 39, L13702, 10.1029/2012gl052107, 2012.

Delworth, T. L., and Zeng, F.: The Impact of the North Atlantic Oscillation on Climate through Its

Influence on the Atlantic Meridional Overturning Circulation, Journal of Climate, 29, 941-962, 10.1175/jcli-d-15-0396.1, 2016.
Ding, Q., and Wang, B.: Circumglobal Teleconnection in the Northern Hemisphere summer, Journal of Climate, 18, 3483-3505, 2005.
Finkenbinder, M. S., Abbott, M. B., and Steinman, B. A.: Holocene climate change in Newfoundland reconstructed using oxygen isotope analysis of lake sediment cores, Global and Planetary Change, 143, 251-261, 10.1016/j.gloplacha.2016.06.014, 2016.
Fisher, D., Osterberg, E., Dyke, A., Dahl-Jensen, D., Demuth, M., Zdanowicz, C., Bourgeois, J., Koerner, R. M., Mayewski, P., Wake, C., Kreutz, K., Steig, E., Zheng, J., Yalcin, K., Goto-Azuma, K., Luckman, B., and Rupper, S.: The Mt Logan Holocene—late Wisconsinan isotope record: tropical Pacific—Yukon connections, The Holocene, 18, 667-677, 10.1177/0959683608092236, 2008.
Fleitmann, D., Burns, S. J., Mangini, A., Mudelsee, M., Kramers, J., Villa, I., Neff, U., Al-Subbary, A. A., Buettner, A., Hippler, D., and Matter, A.: Holocene ITCZ and Indian monsoon dynamics recorded in stalagmites from Oman and Yemen (Socotra), Quaternary Science Reviews, 26, 170-188, 10.1016/j.quascirev.2006.04.012, 2007.
Forman, S., Oglesby, R., Markgraf, V., and Stafford, T.: Paleoclimatic significance of Late Quaternary eolian deposition on the Piedmont and High Plains, Central United States, Global and Planetary Change, 11, 35-55, 1995.
He, F., Shakun, J. D., Clark, P. U., Carlson, A. E., Liu, Z., Otto-Bliesner, B. L., and Kutzbach, J. E.: Northern Hemisphere forcing of Southern Hemisphere climate during the last deglaciation, Nature, 494, 81-85, 10.1038/nature11822, 2013.
He, F.: Simulating Transient Climate Evolution of the Last deglaciation with CCSM3, Doctor of Philosophy, Atmospheric and Oceanic Sciences, University of Wisconsin-Madison, 161 pp., 2011.
Huang, C. C., Pang, J., Zha, X., Su, H., and Jia, Y.: Extraordinary floods related to the climatic event at 4200 a BP on the Qishuihe River, middle reaches of the Yellow River, China, Quaternary Science Reviews, 30, 460-468, 10.1016/j.quascirev.2010.12.007, 2011.
Jansen, E., Overpeck, J. T., Briffa, K. R., Duplessy, J.-C., Joos, F., Masson-Delmotte, V., Olago, D., Otto-Bliesner, B., Peltier, W. R., Rahmstorf, S., Ramesh, R., Raynaud, D., Rind, D. H., Solomina, O., Villalba, R., and Zhang, D.: Palaeoclimate. In: Climate Change 2007: The Physical Science Basis. , Cambridge University Press, Cambridge, United Kingdom and New York, NY, USA, 2007.
Kim, J.-H., Rimbu, N., Lorenz, S. J., Lohmann, G., Nam, S.-I., Schouten, S., Rühlemann, C., and Schneider, R. R.: North Pacific and North Atlantic sea-surface temperature variability during the Holocene, Quaternary Science Reviews, 23, 2141-2154, 10.1016/j.quascirev.2004.08.010, 2004.
Klus, A., Prange, M., Varma, V., Tremblay, L. B., and Schulz, M.: Abrupt cold events in the North Atlantic in a transient Holocene simulation, Climate of the Past Discussions, 1-23, 10.5194/cp-2017-106, 2017.
Kushnir, Y., and Stein, M.: North Atlantic influence on 19th–20th century rainfall in the Dead Sea watershed, teleconnections with the Sahel, and implication for Holocene climate fluctuations, Quaternary Science Reviews, 29, 3843-3860, 10.1016/j.quascirev.2010.09.004, 2010.
Lauritzen, S.-E.: Reconstruction of Holocene climate records from speleothems, in: Global Change

in the Holocene, edited by: Mackay, A., Battarbee, R., Birks, H. J. B., and Oldfield, F., Arnold, London, 242-263, 2003.

Li, J., Sun, C., and Jin, F.-F.: NAO implicated as a predictor of Northern Hemisphere mean temperature multidecadal variability, Geophysical Research Letters, 40, 5497-5502, 10.1002/2013gl057877, 2013.

Lin, J.-S., Wu, B., and Zhou, T.-J.: Is the interdecadal circumglobal teleconnection pattern excited by the Atlantic multidecadal Oscillation?, Atmospheric and Oceanic Science Letters, 9, 451-457, 10.1080/16742834.2016.1233800, 2016.

Liu, J. Q., Lv, H. Y., Negendank, J. F. W., Mingram, J., Luo, X. J., Wang, W. Y., and Chu, G. Q: Cyclic of the Holocene climate variability in Huguangyan Maar lake, China, Chinese Science Bulletin (in Chinese), 45, 1190-1195, 2000.

Liu, Y. H., Sun, X., and Guo, C. Q.: Records of 4.2 ka BP Holocene Event from China and Its Impact on Ancient Civilizations,Geological Science and Technology Information (in Chinese), 32, 99-106, 2013.

Liu, Z. Y., Otto-Bliesner, B., He, F., Brady, E. C., Tomas, R. A., Clark, P. U., Carlson, A. E., Lynch-Stieglitz, J., Curry, W., Brook, E., Erickson, D. J., Jacob, R., Kutzbach, J., and Cheng, J.: Transient simulation of Last Deglaciation with a new mechanism for Bolling-Allerod Warming, Science, 325, 310-314, 2009.

Liu, Z., Carlson, A. E., He, F., Brady, E. C., Otto-Bliesner, B. L., Briegleb, B. P., Wehrenberg, M., Clark, P. U., Wu, S., Cheng, J., Zhang, J., Noone, D., and Zhu, J.: Younger Dryas cooling and the Greenland climate response to CO2, Proceedings of the National Academy of Sciences of the United States of America, 109, 11101-11104, 10.1073/pnas.1202183109, 2012.

Liu, Z., Lu, Z., Wen, X., Otto-Bliesner, B. L., Timmermann, A., and Cobb, K. M.: Evolution and forcing mechanisms of El Nino over the past 21,000 years, Nature, 515, 550-553, 10.1038/nature13963, 2014a.

Liu, Z., Zhu, J., Rosenthal, Y., Zhang, X., Otto-Bliesner, B. L., Timmermann, A., Smith, R. S., Lohmann, G., Zheng, W., and Elison Timm, O.: The Holocene temperature conundrum, Proceedings of the National Academy of Sciences of the United States of America, 111, E3501-3505, 10.1073/pnas.1407229111, 2014b.

Ljung, K., Bjorck, S., Renssen, H., and Hammarlund, D.: South Atlantic island record reveals a South Atlantic response to the 8.2 kyr event, Clim. Past, 4, 35-45, 2008.

Ma, Z. X., Huang, J. H., Wei, Y., Li, J. H., and Hu, C. Y.: Organic carbon isotope records of the Poyang Lake sediments and their implications for the paleoclimate during the last 8 ka, Geochimica (in Chinese), 33, 279-285, 10.19700/j.0379-1726.2004.03.007, 2004.

Marchant, R., and Hooghiemstra, H.: Rapid environmental change in African and South American tropics around 4000 years before present: a review, Earth-Science Reviews, 66, 217-260, 10.1016/j.earscirev.2004.01.003, 2004.

Matero, I. S. O., Gregoire, L. J., Ivanovic, R. F., Tindall, J. C., and Haywood, A. M.: The 8.2 ka cooling event caused by Laurentide ice saddle collapse, Earth and Planetary Science Letters, 473, 205-214, 10.1016/j.epsl.2017.06.011, 2017.

Mayewski, P. A., Rohling, E. E., Curt Stager, J., Karlén, W., Maasch, K. A., Meeker, L. D., Meyerson, E. A., Gasse, F., van Kreveld, S., Holmgren, K., Lee-Thorp, J., Rosqvist, G., Rack, F., Staubwasser, M., Schneider, R. R., and Steig, E. J.: Holocene Climate Variability, Quaternary Research, 62, 243-255, 10.1016/j.yqres.2004.07.001, 2004.

Morrill, C., LeGrande, A. N., Renssen, H., Bakker, P., and Otto-Bliesner, B. L.: Model sensitivity to North Atlantic freshwater forcing at 8.2 ka, Climate of the Past, 9, 955-968, 10.5194/cp-9-955-2013, 2013.

Morrill, C., Ward, E. M., Wagner, A. J., Otto-Bliesner, B. L., and Rosenbloom, N.: Large sensitivity to freshwater forcing location in 8.2 ka simulations, Paleoceanography, 29, 930-945, 10.1002/2014pa002669, 2014.

Nakamura, A., Yokoyama, Y., Maemoku, H., Yagi, H., Okamura, M., Matsuoka, H., Miyake, N., Osada, T., Adhikari, D. P., Dangol, V., Ikehara, M., Miyairi, Y., and Matsuzaki, H.: Weak monsoon event at 4.2 ka recorded in sediment from Lake Rara, Himalayas, Quaternary International, 397, 349-359, 10.1016/j.quaint.2015.05.053, 2016.

Ning, L., Liu, J., Bradley, R. S., and Yan, M.: Comparing the spatial patterns of climate change in the 9th and 5th millennia BP from TRACE-21 model simulations, Climate of the Past, 15, 41-52, 10.5194/cp-15-41-2019, 2019.

Owen, L. A., and Dortch, J. M.: Nature and timing of Quaternary glaciation in the Himalayan–Tibetan orogen, Quaternary Science Reviews, 88, 14-54, 10.1016/j.quascirev.2013.11.016, 2014.

Peltier, W. R.: GLOBAL GLACIAL ISOSTASY AND THE SURFACE OF THE ICE-AGE EARTH: The ICE-5G (VM2) Model and GRACE, Annual Review of Earth and Planetary Sciences, 32, 111-149, 10.1146/annurev.earth.32.082503.144359, 2004.

Peng, Y., Xiao, J., Nakamura, T., Liu, B., and Inouchi, Y.: Holocene East Asian monsoonal precipitation pattern revealed by grain-size distribution of core sediments of Daihai Lake in Inner Mongolia of north-central China, Earth and Planetary Science Letters, 233, 467-479, 10.1016/j.epsl.2005.02.022, 2005.

Ramos-Román, M. J., Jiménez-Moreno, G., Camuera, J., García-Alix, A., Anderson, R. S., Jiménez-Espejo, F. J., and Carrión, J. S.: Holocene climate aridification trend and human impact interrupted by millennial- and centennial-scale climate fluctuations from a new sedimentary record from Padul (Sierra Nevada, southern Iberian Peninsula), Climate of the Past, 14, 117-137, 10.5194/cp-14-117-2018, 2018.

Rimbu, N., Lohmann, G., Lorenz, S. J., Kim, J. H., and Schneider, R. R.: Holocene climate variability as derived from alkenone sea surface temperature and coupled ocean-atmosphere model experiments, Climate Dynamics, 23, 215-227, 10.1007/s00382-004-0435-8, 2004.

Roland, T. P., Caseldine, C. J., Charman, D. J., Turney, C. S. M., and Amesbury, M. J.: Was there a ‘4.2 ka event’ in Great Britain and Ireland? Evidence from the peatland record, Quaternary Science Reviews, 83, 11-27, 10.1016/j.quascirev.2013.10.024, 2014.

Rupper, S., Roe, G., and Gillespie, A.: Spatial patterns of Holocene glacier advance and retreat in Central Asia, Quaternary Research, 72, 337-346, 10.1016/j.yqres.2009.03.007, 2009.

Sachs, J. P.: Cooling of Northwest Atlantic slope waters during the Holocene, Geophysical Research Letters, 34, L03609, 10.1029/2006gl028495, 2007.

Shakun, J. D., Clark, P. U., He, F., Marcott, S. A., Mix, A. C., Liu, Z., Otto-Bliesner, B., Schmittner, A., and Bard, E.: Global warming preceded by increasing carbon dioxide concentrations during the last deglaciation, Nature, 484, 49-54, 10.1038/nature10915, 2012.

Shanahan, T. M., Overpeck, J. T., Anchukaitis, K. J., Beck, J. W., Cole, J. E., Dettman, D. L., Peck, J. A., Scholz, C. A., and King, J. W.: Atlantic forcing of persistent drought in West Africa, Science, 324, 377-380, 2009.

Sigl, M., Severi, M., and McConnell, J. R.: A role for volcanoes in causing the "4.2 ka BP event"?, The 4.2 ka BP event: an international workshop, Pisa, Italy, 2018.

Solomina, O. N., Bradley, R. S., Hodgson, D. A., Ivy-Ochs, S., Jomelli, V., Mackintosh, A. N., Nesje, A., Owen, L. A., Wanner, H., Wiles, G. C., and Young, N. E.: Holocene glacier fluctuations, Quaternary Science Reviews, 111, 9-34, 10.1016/j.quascirev.2014.11.018, 2015.

Staubwasser, M., and Weiss, H.: Holocene Climate and Cultural Evolution in Late Prehistoric–Early Historic West Asia, Quaternary Research, 66, 372-387, 10.1016/j.yqres.2006.09.001, 2006.

Staubwasser, M., Sirocko, F., Grootes, P. M., and Segl, M.: Climate change at the 4.2 ka BP termination of the Indus valley civilization and Holocene south Asian monsoon variability, Geophysical Research Letters, 30, No. 8, 1425, 10.1029/2002gl016822, 2003.

Tan, L. C., An, Z. S., Cai, Y. J., and Long, H.: The Hydrological Exhibition of 4.2 ka BP Event in China and Its Global Linkages, Geological Review (in Chinese), 54, 94-104, 10.16509/j.georeview.2008.01.010, 2008.

Tan, L. C., Cai, Y. J., Cheng, H., Edwards, L. R., Gao, Y. L., Xu, H., Zhang, H. W., and An, Z. S.: Centennial- to decadal- scale monsoon precipitation variations in the upper Hanjiang River region, China over the past 6650 years, Earth and Planetary Science Letters, 482, 580-590, 10.1016/j.epsl.2017.11.044, 2018.

Thompson, L. G., Mosley-Thompson, E., Davis, M., Henderson, K. A., Brecher, H., Zagorodnov, V. S., Mashiotta, T., Lin, P. N., Mikhalenko, V. N., Hardy, D. R., and Beer, J.: Kilimanjara Ice Core Records: Evidence of Holocene Climate Change in Tropical Africa, Science, 298, 589-593, 10.1126/science.1073198, 2002.

Tremblay, L. B., Mysak, L. A., and Dyke, A. S.: Evidence from driftwood records for century-to-millennial scale variations of the high latitude atmospheric circulation during the Holocene, Geophysical Research Letters, 24, 2027-2030, 10.1029/97gl02028, 1997.

Turney, C., Baillie, M., Clemens, S., Brown, D., Palmer, J., Pilcher, J., Reimer, P., and Leuschner, H. H.: Testing solar forcing of pervasive Holocene climate cycles, Journal of Quaternary Science, 20, 511-518, 10.1002/jqs.927, 2005.

Vellinga, M., and Wood, R. A.: Global climatic impacts of a collapse of the Atlantic Thermohaline Circulation, Climatic Change, 54, 251-267, 2002.

Wagner, A. J., Morrill, C., Otto-Bliesner, B. L., Rosenbloom, N., and Watkins, K. R.: Model support for forcing of the 8.2 ka event by meltwater from the Hudson Bay ice dome, Climate Dynamics, 41, 2855-2873, 10.1007/s00382-013-1706-z, 2013.

Walker, M. J. C., Berkelhammer, M., Björck, S., Cwynar, L. C., Fisher, D. A., Long, A. J., Lowe, J. J., Newnham, R. M., Rasmussen, S. O., and Weiss, H.: Formal subdivision of the Holocene Series/Epoch: a Discussion Paper by a Working Group of INTIMATE (Integration of ice-core, marine and terrestrial records) and the Subcommission on Quaternary Stratigraphy (International Commission on Stratigraphy), Journal of Quaternary Science, 27, 649-659, 10.1002/jqs.2565, 2012.

Wang, S. W.: 4.2ka BP Event, Advances in Climate Change Research (in Chinese), 6, 75-76, 2010.

Wang, S. W.: Holocene cold events in the North Atlantic: Chronology and Climate Impact, Quaternary Sciences (in Chinese), 29, 1146-1153, 2009.

Wang, Y. J., Cheng, H., Edwards, L. R., He, Y. Q., Kong, X. G., An, Z. S., Wu, J. Y., Kelly, M., Dykoski, C. A., and Li, X. D.: The Holocene Asian Monsoon: Links to Solar Changes and North Atlantic Climate, Science, 308, 854-857, 2005.

Wanner, H., Beer, J., Bütikofer, J., Crowley, T. J., Cubasch, U., Flückiger, J., Goosse, H., Grosjean, M., Joos, F., Kaplan, J. O., Küttel, M., Müller, S. A., Prentice, I. C., Solomina, O., Stocker, T. F., Tarasov, P., Wagner, M., and Widmann, M.: Mid- to Late Holocene climate change: an overview, Quaternary Science Reviews, 27, 1791-1828, 10.1016/j.quascirev.2008.06.013, 2008.

Weiss, H., and Bradley, R. S.: What drives societal collapse?, Science, 291, 609-610, 2001.

Weiss, H., Courty, M. A., Wetterstrom, W., Guichard, F., Senior, L., Meadow, R., and Curnow, A.: The Genesis and Collapse of Third Millennium North Mesopotamian Civilization, Science, 261, 995-1004, 10.1126/science.261.5124.995, 1993.

Weiss, H.: Global megadrought, societal collapse and resilience at 4.2-3.9 ka BP across the Mediterranean and west Asia, Past Global Change Magazine, 24, 62-63, 10.22498/pages.24.2.62, 2016.

Weiss, H.: Megadrought, Collapse, and Resilience in late 3rd millennium BC Mesopotamia, 7th Archaeological Conference of Central Germany, Halle (Saale), 2015.

Wu, W. X., and Liu T. S.: 4000aB.P. Event and its implications for the origin of Ancient Chinese Civilization, Quaternary Sciences (in Chinese), 21, 443-451, 2001.

Wu, W. X., and Liu, T. S.: Possible role of the "Holocene Event 3" on the collapse of Neolithic Cultures around the Central Plain of China, Quaternary International, 117, 153-166, 10.1016/s1040-6182(03)00125-3, 2004.

Yang, X. P., Scuder, L. A., Wang, X. L., Scuder, L. J., Zhang, D. G., Li, H. W., and al, e.: Groundwater sapping as the cause of irreversible desertification of Hunshandake Sandy Lands, Inner Mongolia, northern China, PNAS, 112, 702-706, 2015.

Yechieli, Y., Magaritz, M., Levy, Y., Weber, U., Kafri, U., Woelfli, W., and Bonani, G.: Late Quaternary Geological History of the Dead Sea Area, Israel, Quaternary Research, 39, 59-67, 10.1006/qres.1993.1007, 1993.

Zhang, R., and Delworth, T. L.: Simulated Tropical Response to a Substantial Weakening of the Atlantic Thermahaline Circulation, Journal of Climate, 18, 1853-1860, 2005.

Zhang, R., and Delworth, T. L.: Impact of Atlantic multidecadal oscillations on India/Sahel rainfall and Atlantic hurricanes, Geophysical Research Letters, 33, L17712, 10.1029/2006gl026267, 2006.

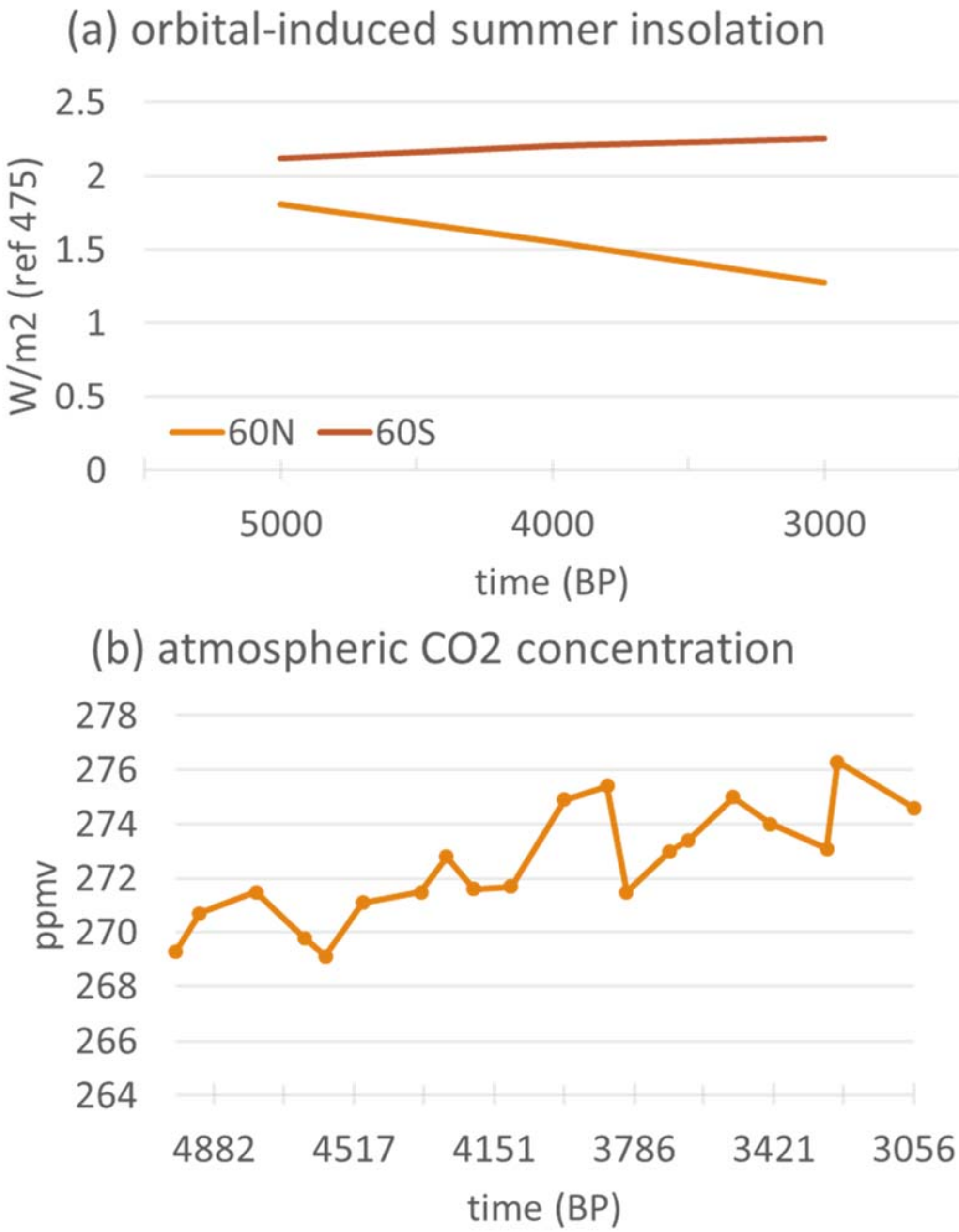

Figure 1 Time series of (a) transient summer insolation (at 60°N and 60°S) changes resulted from the orbital variation and (b) the transient CO_2 change used in the simulations.

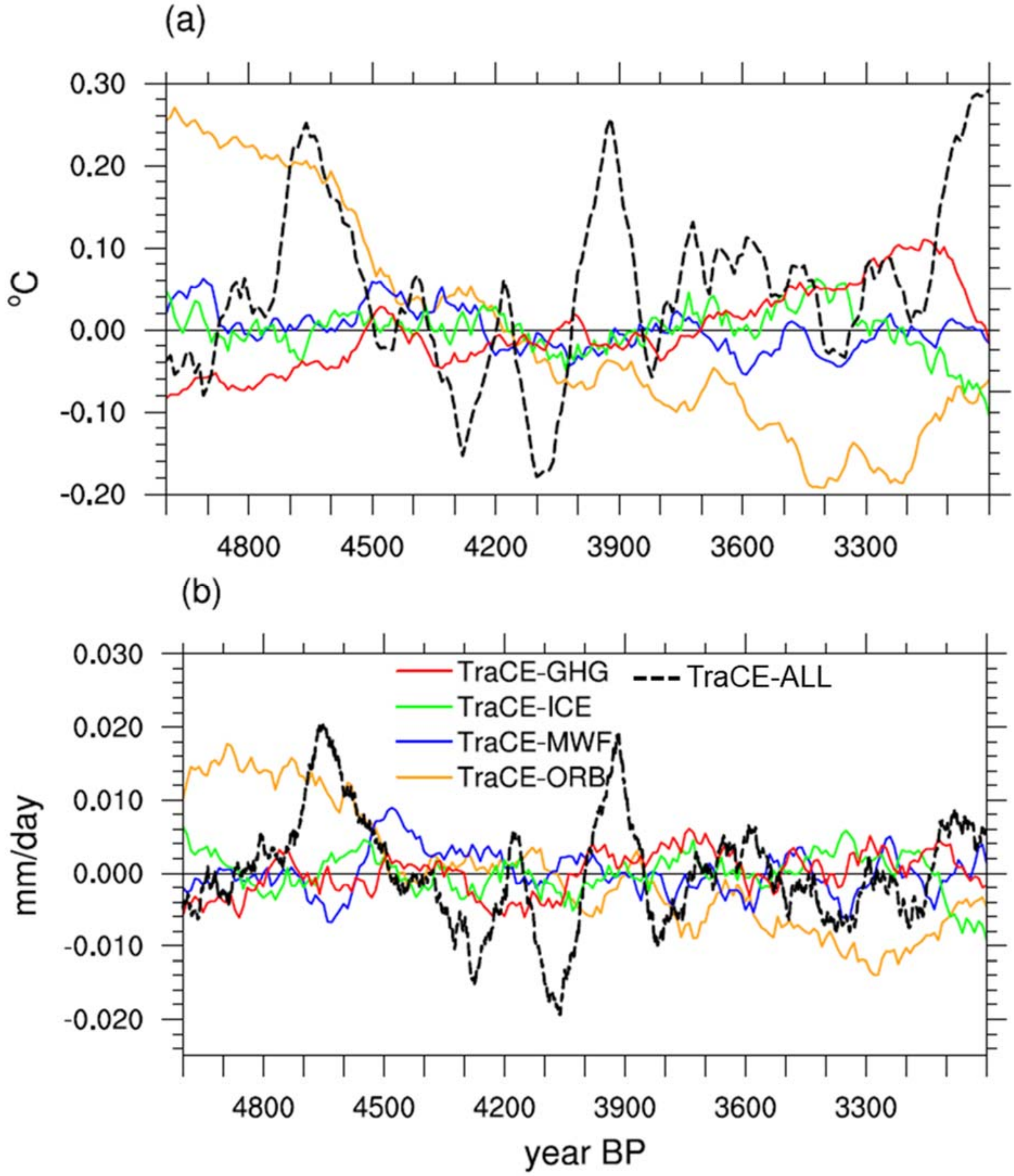

Figure 2 Time series of annual mean NH (a) surface temperature anomalies and (b) precipitation anomalies derived from the TraCE-ALL run (dashed black lines) and each single forcing runs (solid color lines) from 5 ka BP to 3 ka BP. A 101-year running mean has been applied to the time series.

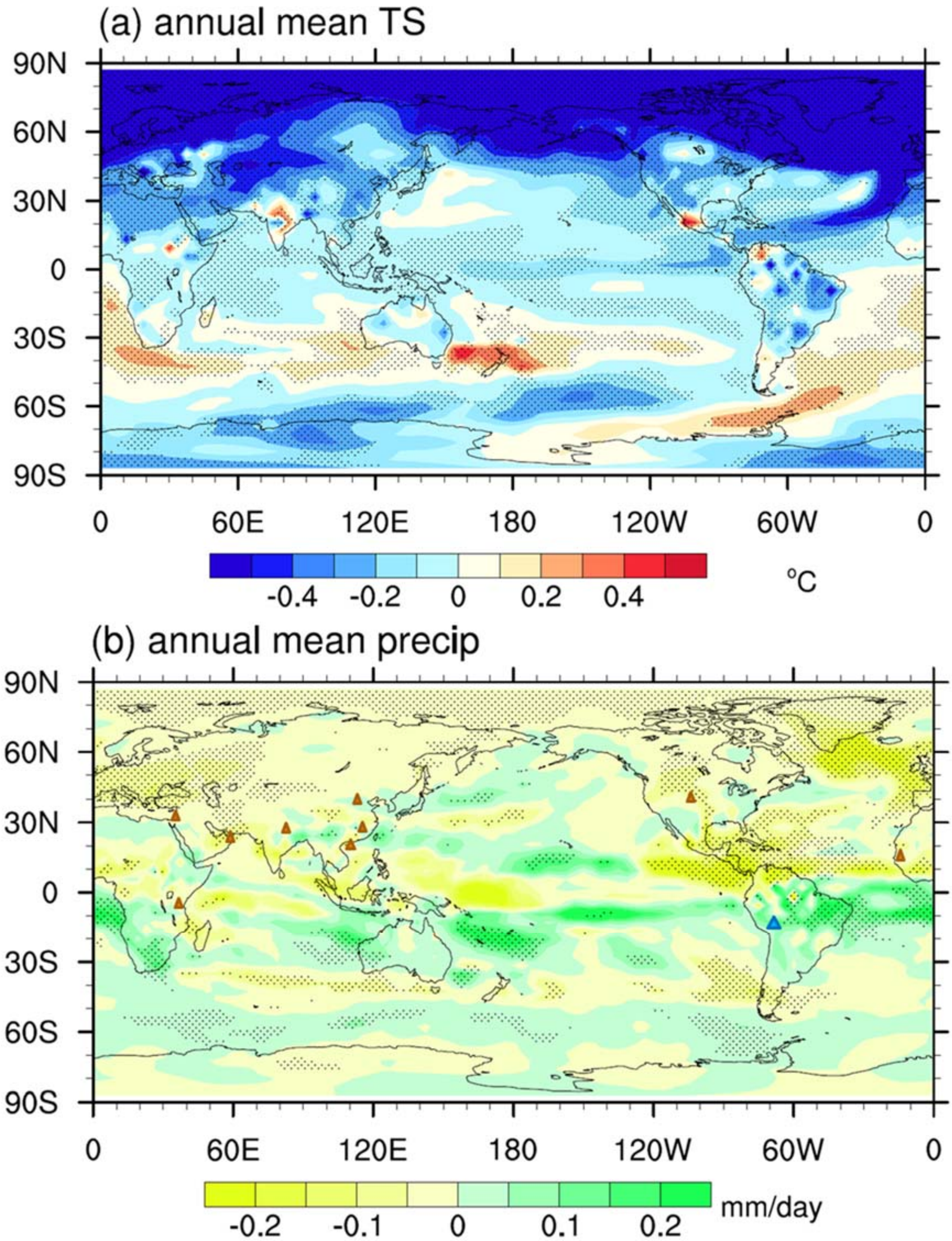

Figure 3 Spatial distribution of the annual mean (a) surface temperature and (b) precipitation differences between the cold periods and warm periods derived from the TraCE-ALL run. Those regions where significant above 95% confidence level are dotted. Triangles in (b) denote the dry (orange) and wet (blue) conditions documented

in the records, including the following sites: Kilimanjaro (3°04.6’S, 37°21.2’E) (Thompson et al., 2002), Dead Sea (Yechieli et al., 1993), Gulf of ~~Omen~~ Oman (24°23.4’N, 59°2.5’E) (Cullen et al., 2000), Lake Rara (29°32’N, 82°05’E) (Nakamura et al., 2016), Maar lake in Huguangyan (21.15°N, 110.29°E) (Liu et al., 2000), Daihai Lake (40.58°N, 112.7°E) (Peng et al., 2005), Poyang Lake (29.15°N, 116.27°E) (Ma et al., 2004), Eastern Colorado Dunes (40°20’N, 104°16’E) (Forman et al., 1995), Lake Titicaca (12.08°S, 69.85°W) and Lake Guiers (16.3°N, 16.5°W) (Marchant and Hooghiemstra, 2004).

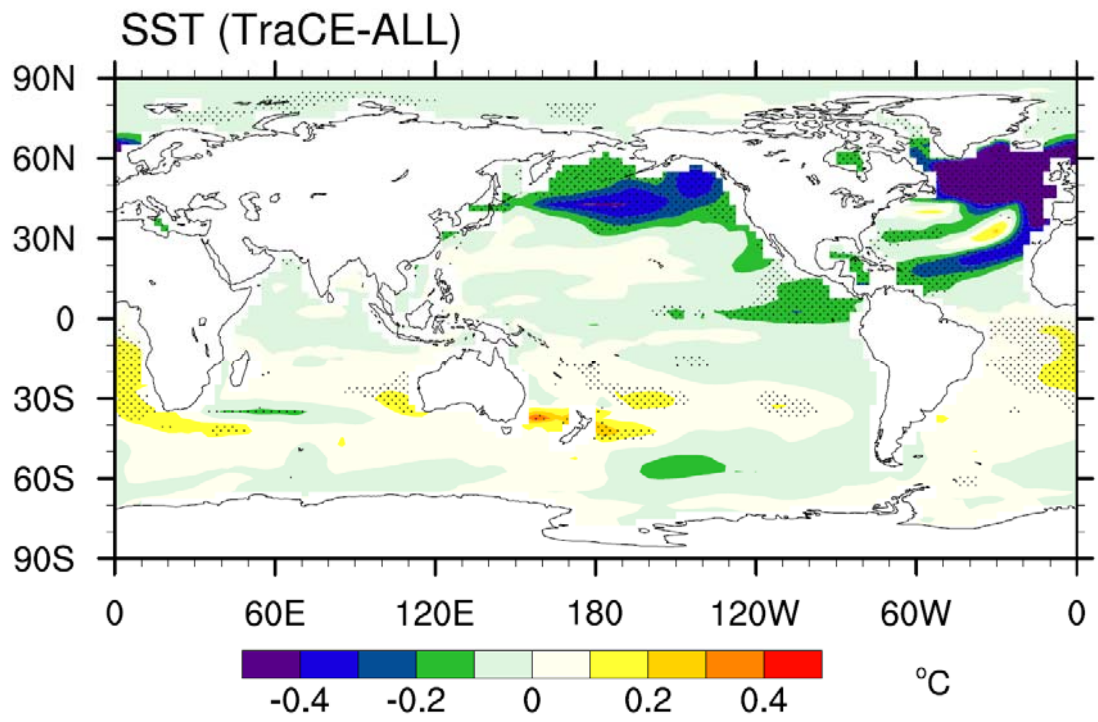

Figure 4 Spatial distribution of annual mean SST difference between the cold and warm periods derived from the TraCE-ALL run. Those regions where significant above 95% confidence level are dotted.

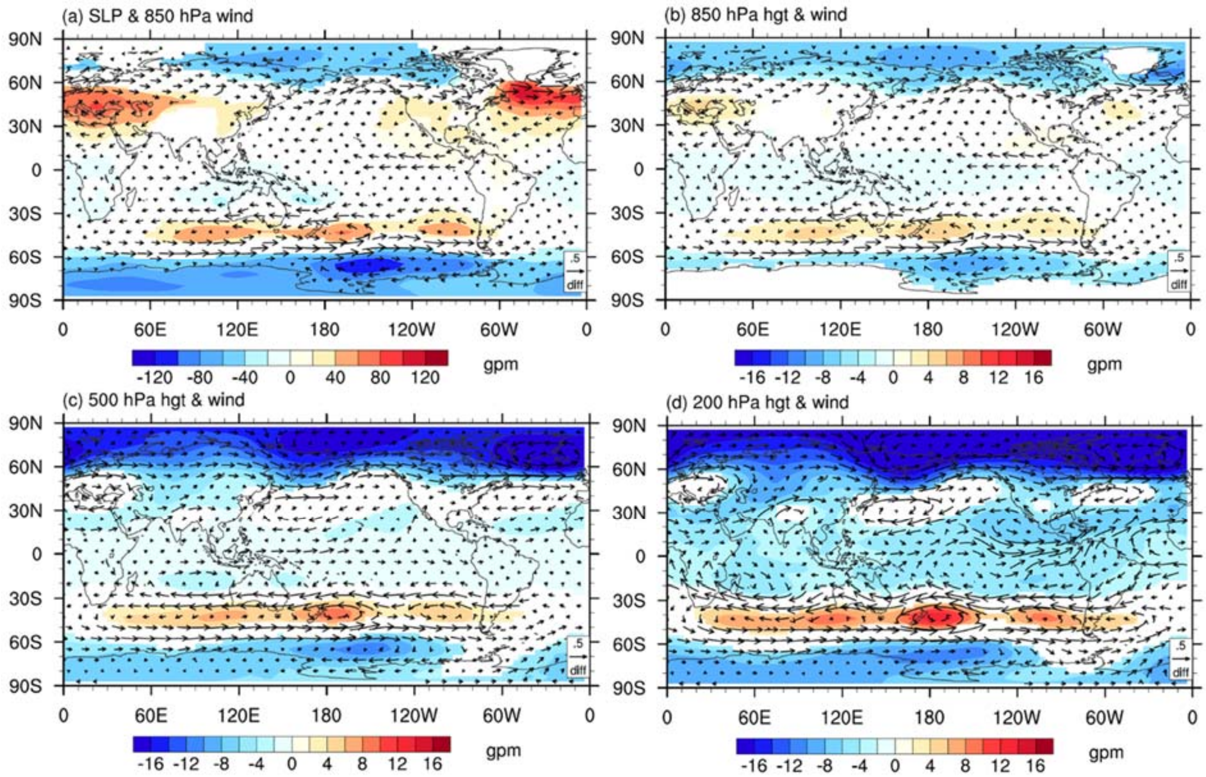

Figure 5 Differences of annual mean (a) sea level pressure and 850 hPa wind, (b) geopotential height and wind on 850 hPa, (c) geopotential height and wind on 500 hPa and (d) geopotential height and wind on 200 hPa between cold and warm periods derived from the TraCE-ALL run. Those regions where significant above 95% confidence level are plotted.

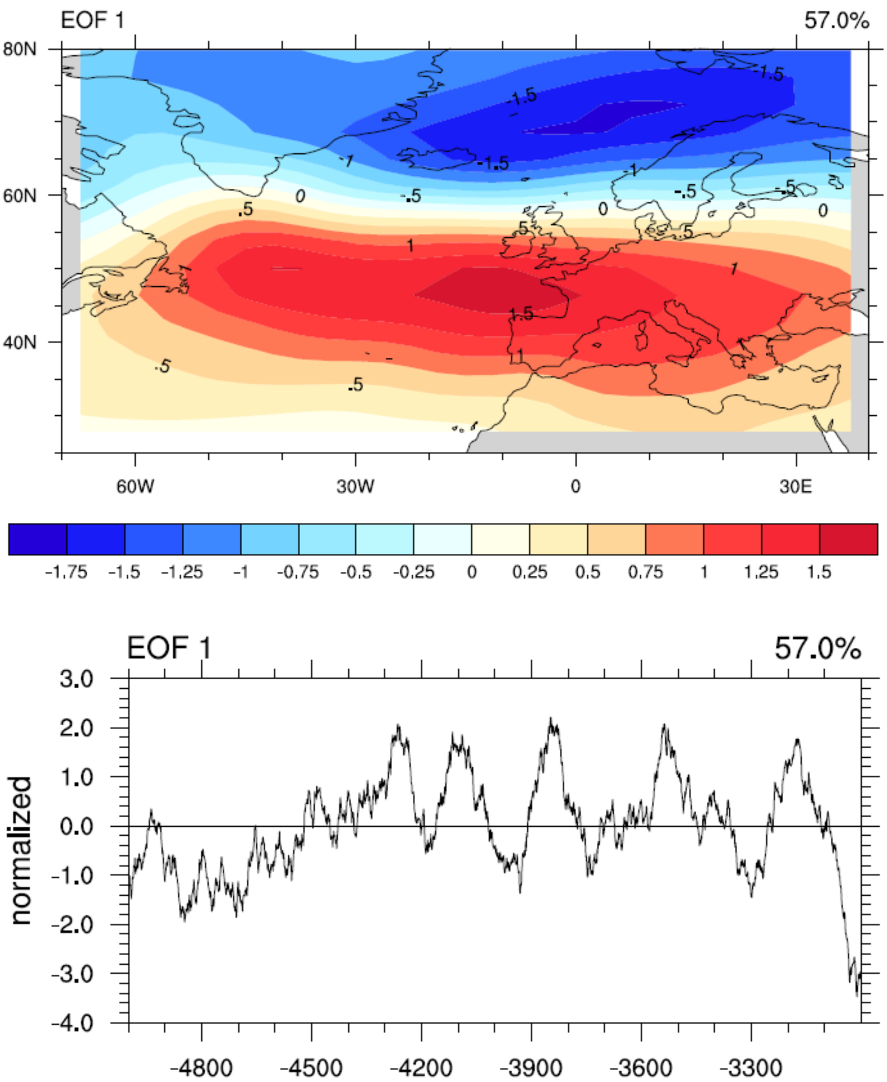

Figure 6 Standardized first leading mode of the EOF of annual mean SLP over the North Atlantic region (70W-40E, 25N-80N) during the period of 5.0 ka BP to 3.0 ka BP derived from the TraCE-ALL run, after application of a 101-year running mean. The spatial distribution is shown in the top panel, and the time series is shown in the bottom panel. Only this mode passed the North test for EOF.

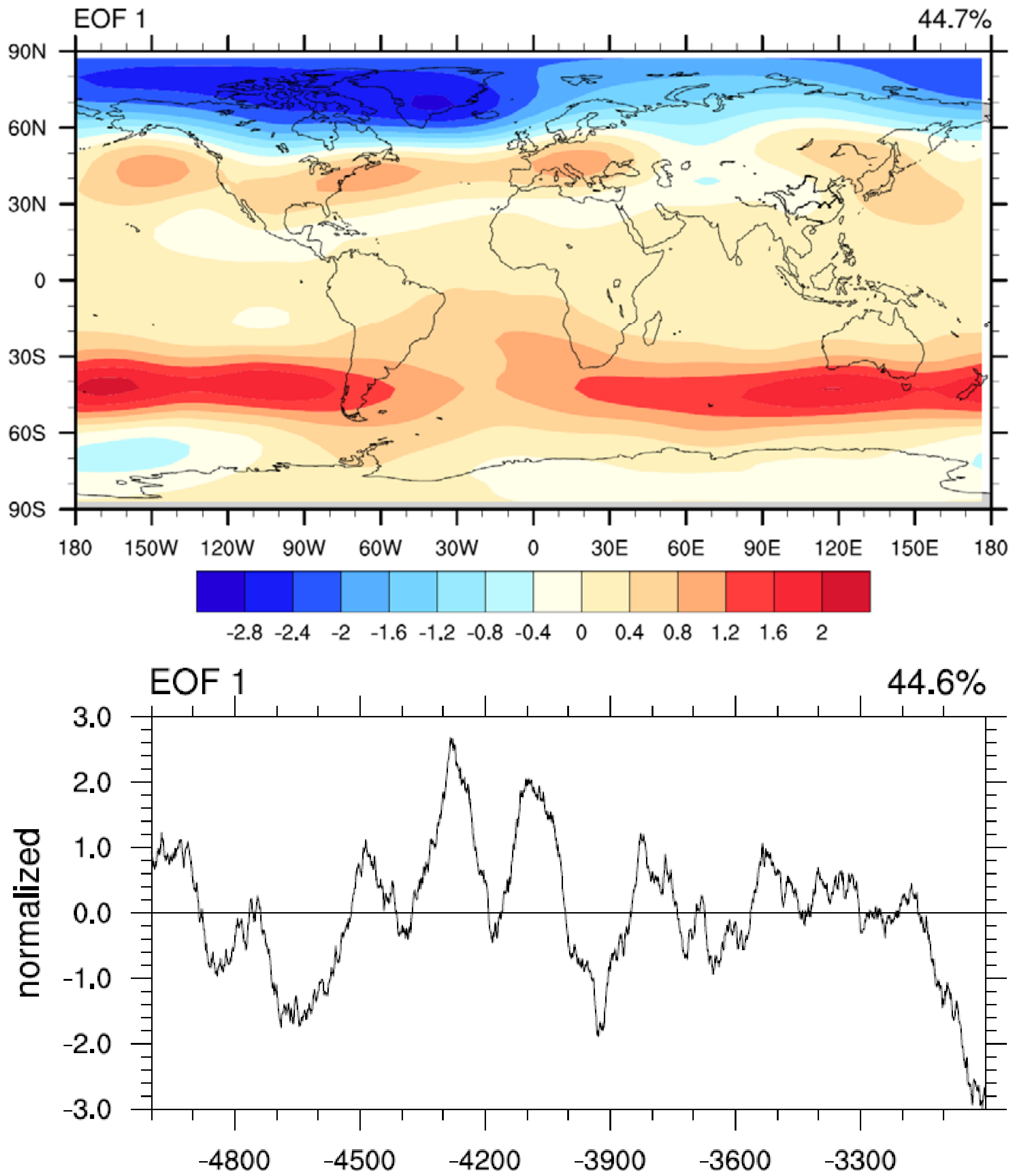

Figure 7 Standardized first leading mode of the EOF of annual mean geopotential height at 200 hPa during the period of 5.0 ka BP to 3.0 ka BP derived from the TraCE-ALL run, after application of a 101-year running mean. The spatial distribution is shown in the top panel, and the time series is shown in the bottom panel. Only this mode passed the North test for EOF.

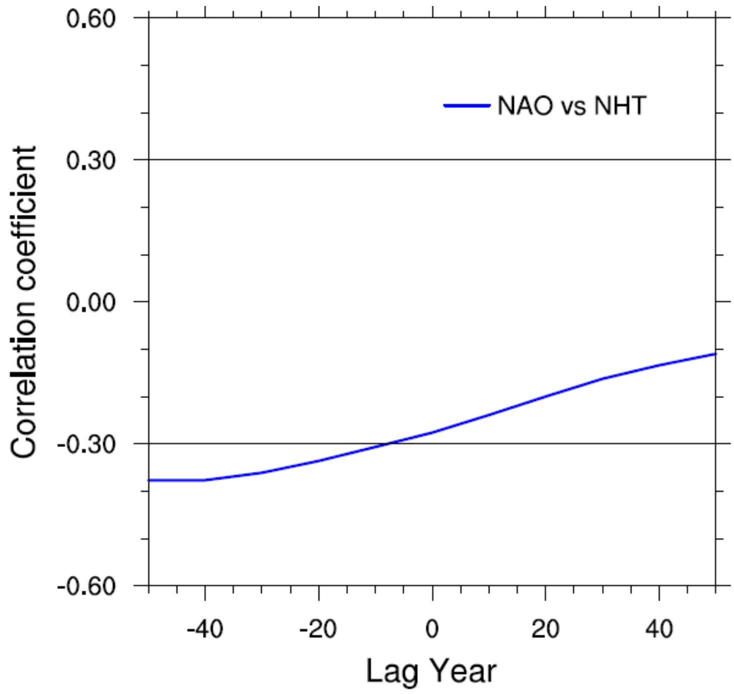

Figure 8 Lead-lag correlation between the annual mean North Atlantic Oscillation (NAO) and the North Hemisphere Surface Temperature (NHT) during 4.4 ka BP-4.0 ka BP derived from the TraCE-ALL run. The black lines (±0.3) show the significance levels ($p<0.05$).

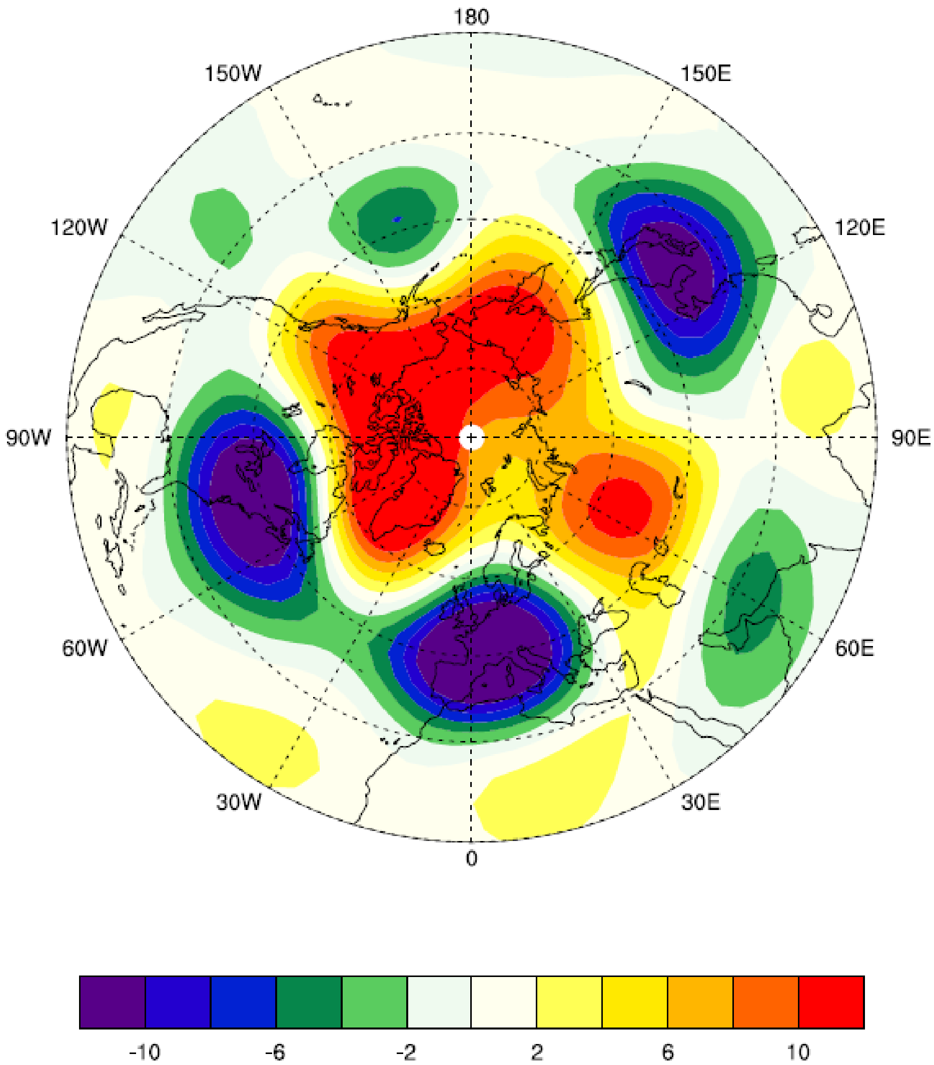

Figure 9 Annual mean geopotential height regressed against the SST over the North Atlantic during 5.0 ka BP - 3.0 ka BP derived from the TraCE-ALL run, after 31-year running mean application.

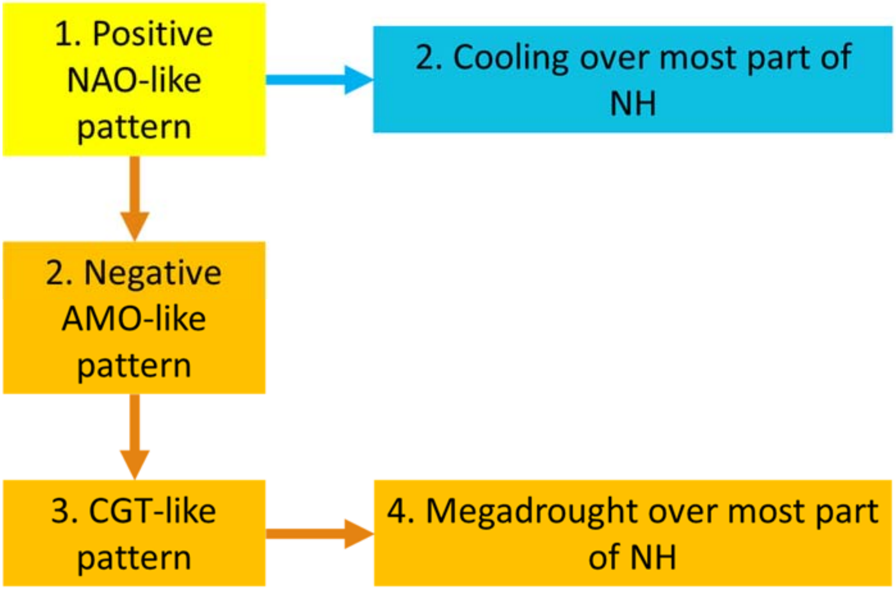

Figure 10 Schematic diagram shown the mechanisms behind the 4.2 ka BP event.

Table 1 The information of the experiments used in this study.

Experiments	Forcings	Time spanning	Temporal resolution
TraCE-ALL	Orbital, melt-water flux, continental ice-sheet, and Greenhouse gases	22000 BP to 1990 CE	Monthly mean
TraCE-ORB	Orbital only	22000 BP to 1990 CE	Decadal mean
TraCE-MWF	Melt-water flux only	19000 BP to 1990 CE	Decadal mean
TraCE-ICE	Continental ice-sheets only	19000 BP to 1990 CE	Decadal mean
TraCE-GHG	Greenhouse gases only	22000 BP to 1990 CE	Decadal mean

Table 2 Correlation coefficients between the annual mean and seasonal mean NHTs derived from the TraCE-ALL run and those from each single-forcing run from 5.0 ka BP to 3.0 ka BP.

Single forcing run	Annual mean	JJA mean	DJF mean
TraCE-ORB	-0.05	0.79	-0.12
TraCE-MWF	-0.18	0.48	-0.43
TraCE-ICE	-0.30	-0.20	-0.18
TraCE-GHG	0.14	-0.73	0.40

Supplementary Information for

Physical processes of cooling and megadrought in 4.2 ka BP event: results from TraCE-21ka simulations

Mi Yan[1,2], Jian Liu[1,2,3*]

[1]Key Laboratory for Virtual Geographic Environment of Ministry of Education/State Key Laboratory of Geographical Evolution of Jiangsu Provincial Cultivation Base/School of Geography Science, Jiangsu Center for Collaborative Innovation in Geographical Information Resource Development and Application, Nanjing Normal University, Nanjing 210023, China

[2]Open Studio for the Simulation of Ocean-Climate-Isotope, Pilot National Laboratory for Marine Science and Technology, Qingdao 266237, China

[3]Jiangsu Provincial Key Laboratory for Numerical Simulation of Large Scale Complex Systems/School of Mathematical Science, Nanjing Normal UniversityKey Laboratory of Virtual Geographic Environment, Ministry of Education; State key Laboratory of Geographical Environment Evolution, Jiangsu Provincial Cultivation Base; School of Geographical Science, Nanjing Normal University, Nanjing, 210023, China

[2]Jiangsu Center for Collaborative Innovation in Geographical Information Resource Development and Application, Nanjing, 210023, China

[*]jliu@njnu.edu.cn

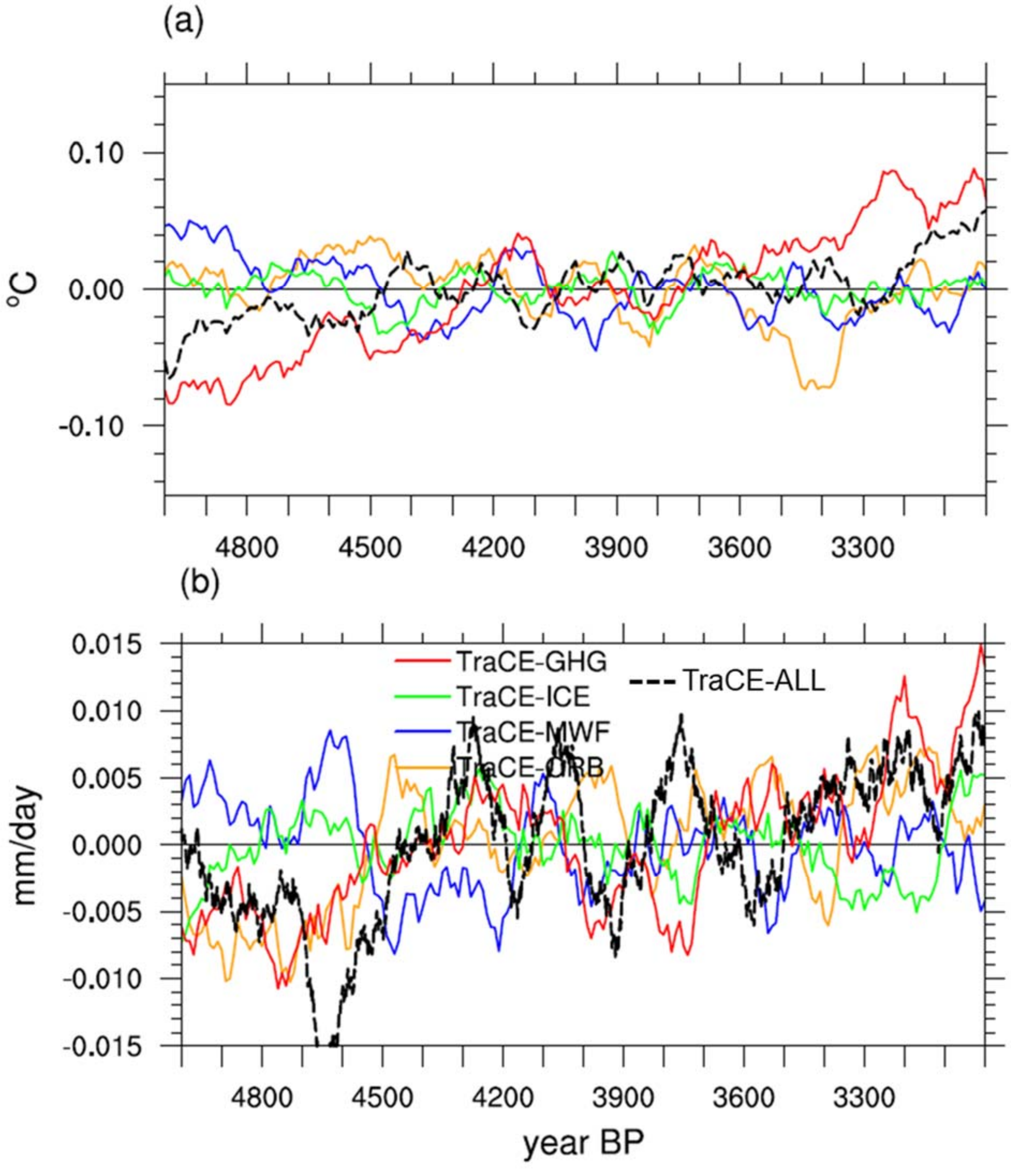

Figure S1 Time series of annual mean Southern Hemisphere (SH) (a) surface temperature anomalies and (b) precipitation anomalies derived from TraCE-ALL run (dashed black lines) and each single forcing runs (solid color lines) from 5 ka BP to 3 ka BP. A 101-year running mean has been applied to the time series.

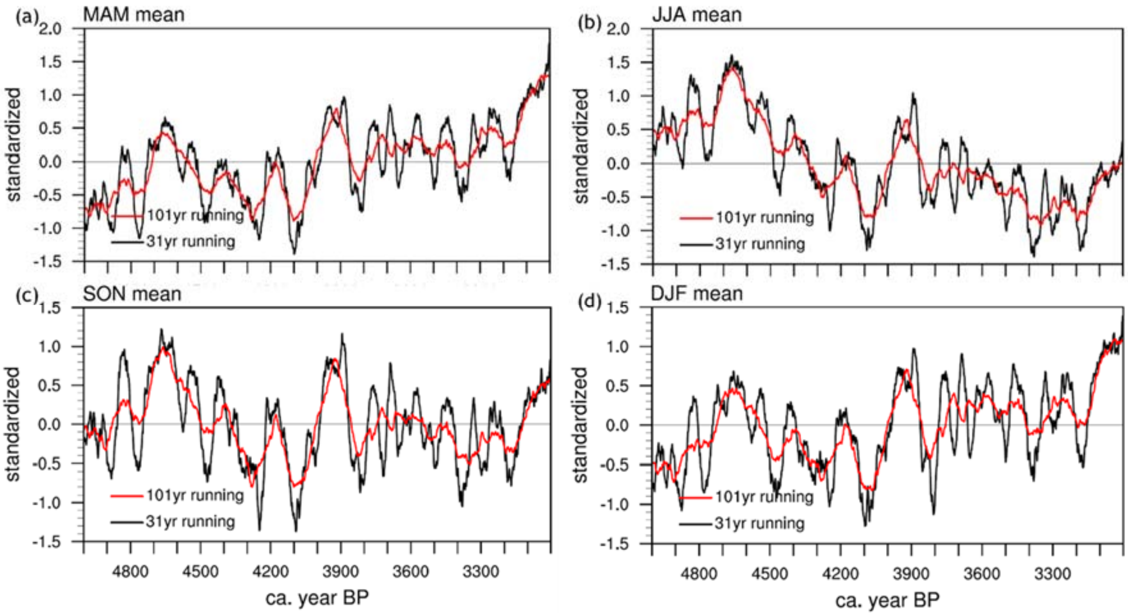

Figure S2 Standardized time series of (a) MAM mean, (b) JJA mean, (c) SON mean and (d) DJF mean NH surface temperature anomalies from 5ka BP to 3ka BP derived from the TraCE-ALL run. A 101-year running mean (red line) and a 31-year running mean (black line) have been applied to the time series.

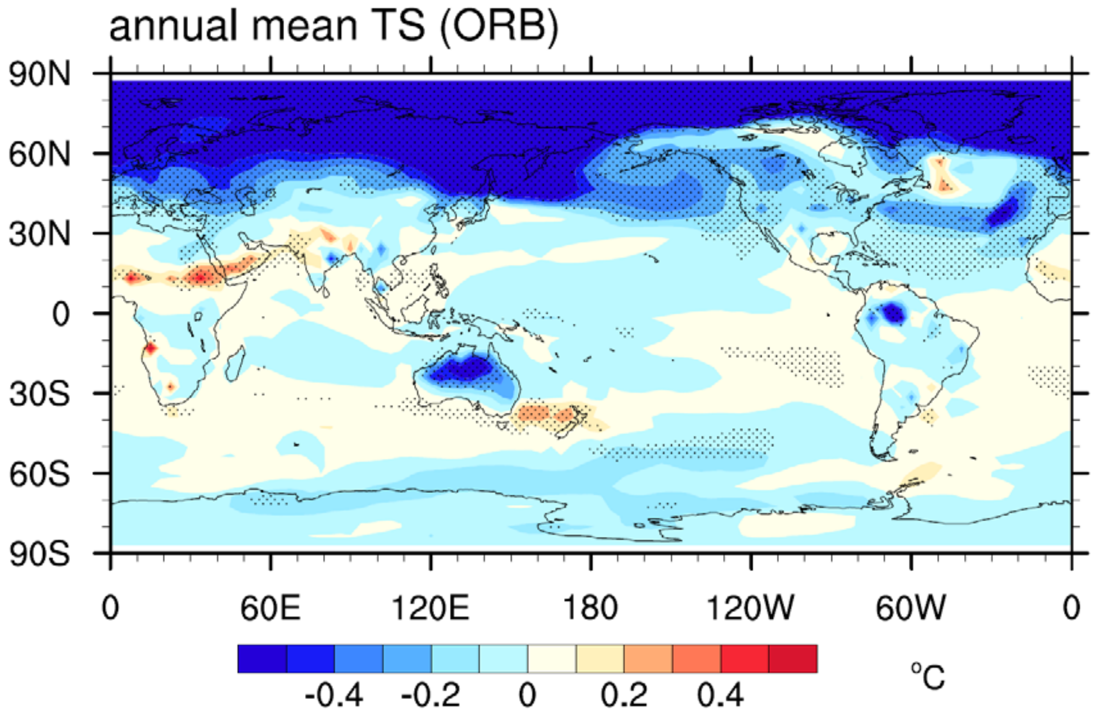

Figure S3 Spatial distribution of the annual mean surface temperature difference between the cold period (4200 BP-3900 BP) and warm period (4800 BP-4500 BP) derived from the TraCE-ORB run. Those regions where significant above 95% confidence level are dotted.

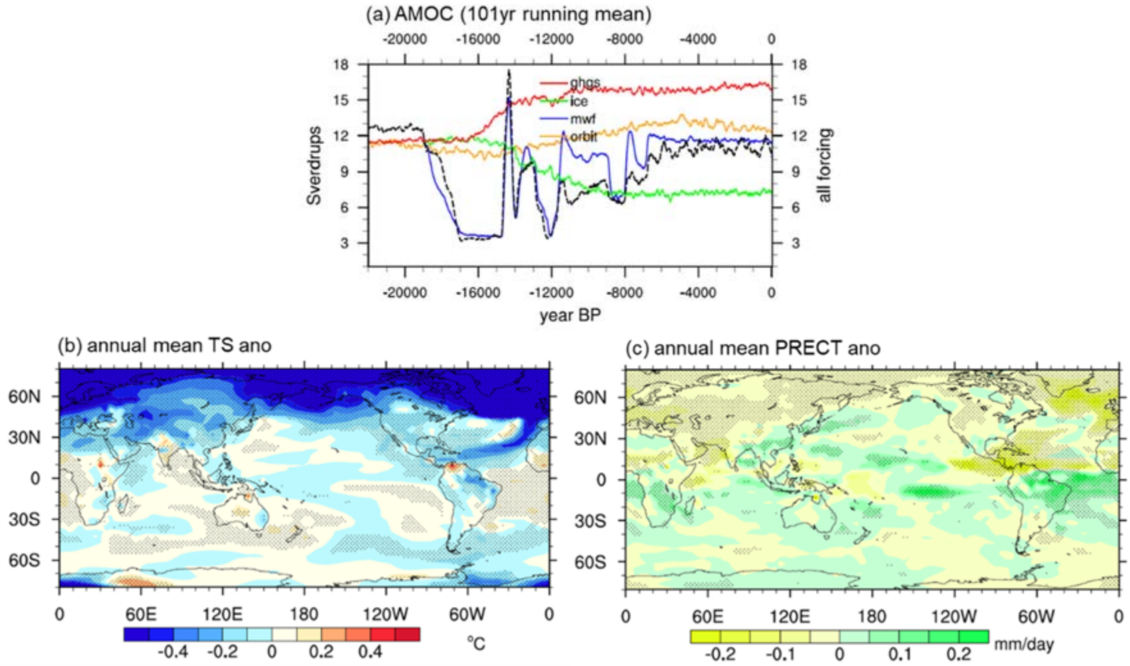

Figure S4 (a) Simulated AMOC over the past 22 ka derived from TraCE-ALL (black line) and each single forcing run (colored lines). Spatial distribution of the annual mean surface temperature difference (b) and precipitation difference (c) between the weak and strong AMOC states derived from TraCE-ALL. Those regions where significant above 95% confidence level are dotted in (b) and (c).
The weak and strong AMOC states are selected based on the standardized time series of AMOC during the period of past 6 ka, when the meltwater forcing is absent.

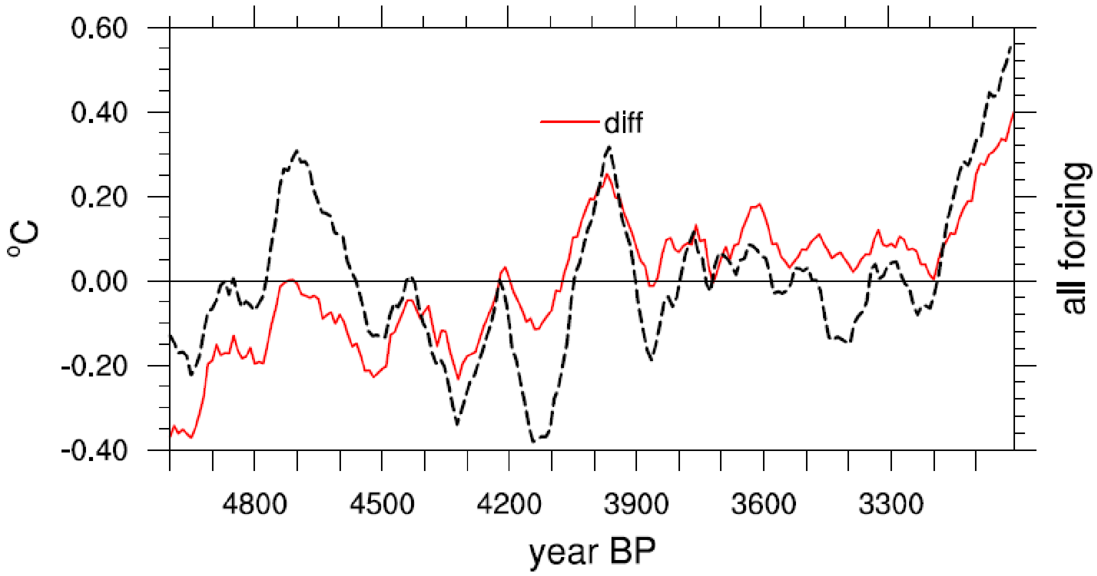

Figure S5 Time series of annual mean NHT anomaly from 5000 BP to 3000 BP. Dashed black line is the result derived from the all forcing run. Red line indicates the difference between the result derived from all forcing run and that derived from the linear sum of the 4 single forcing runs.

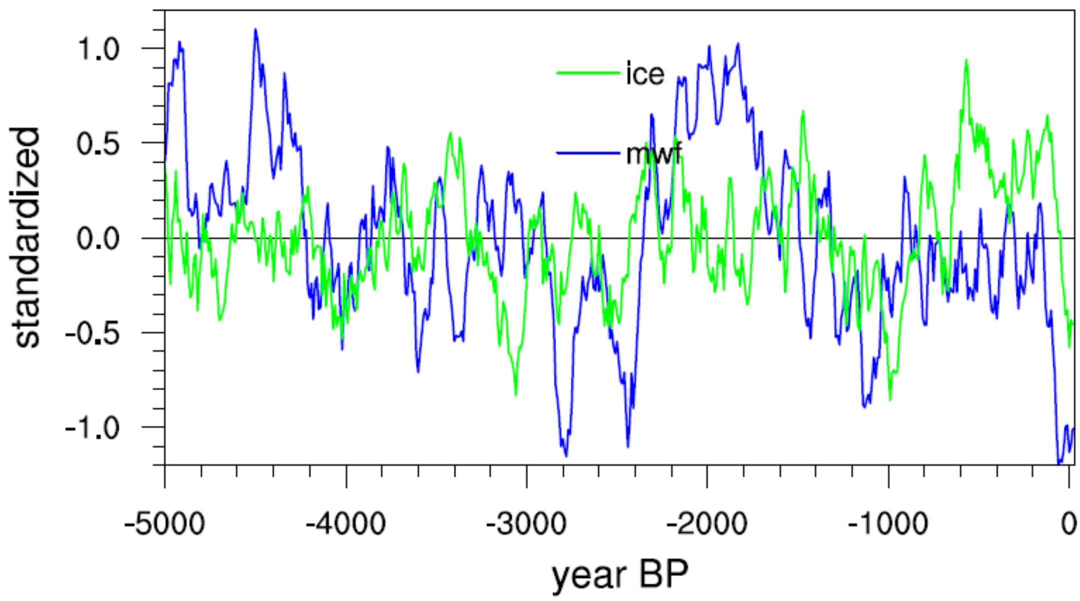

Figure S6 Standardized time series of the annual mean NHT derived from the TraCE-MWF run (blue line) and TraCE-ICE run (green line) from 5000 BP to 1990 CE. A 101-year running mean has been applied to the time series.

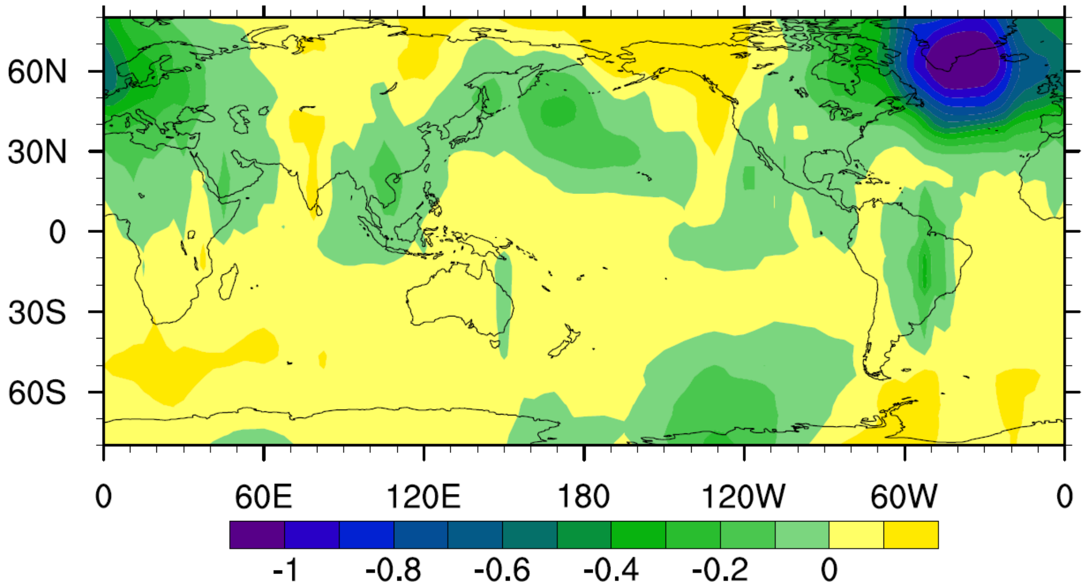

Figure S7 Annual mean TS regressed against the NAO index leading 40-year during 4.4 ka BP - 4.0 ka BP.